

AUTOMATED DETECTION OF SLEEP SPINDLES

A THESIS SUBMITTED TO
THE GRADUATE SCHOOL OF NATURAL AND APPLIED SCIENCES
OF
THE MIDDLE EAST TECHNICAL UNIVERSITY

BY

DILAN GÖRÜR

IN PARTIAL FULFILLMENT OF THE REQUIREMENTS FOR THE DEGREE OF
MASTER OF SCIENCE
IN
THE DEPARTMENT OF ELECTRICAL AND ELECTRONICS ENGINEERING

JANUARY 2003

Approval of the Graduate School of Natural and Applied Sciences

Prof. Dr. Tayfur Öztürk
Director

I certify that this thesis satisfies all the requirements as a thesis for the degree of Master of Science.

Prof. Dr. Mübeccel Demirekler
Head of Department

This is to certify that we have read this thesis and that in our opinion it is fully adequate, in scope and quality, as a thesis for the degree of Master of Science.

Prof. Dr. Uğur Halıcı
Co-Supervisor

Assoc.Prof. Dr.
Nevzat G. Gençer
Supervisor

Examining Committee Members

Prof. Dr. Kemal Leblebicioğlu

Assoc. Prof. Dr. Nevzat G. Gençer

Prof. Dr. Uğur Halıcı

Prof. Dr. Hamdullah Aydın

Assoc. Prof. Dr. Volkan Atalay

ABSTRACT

AUTOMATED DETECTION OF SLEEP SPINDLES

Görür, Dilan

DEPARTMENT OF ELECTRICAL AND ELECTRONICS ENGINEERING

Supervisor: Assoc. Prof. Dr. Nevzat G. Gençer

Co- Supervisor: Prof. Dr. Uğur Halıcı

January 2003, 72 pages

Sleep spindles are one of the rhythmic activities observed in sleep electroencephalogram (EEG). As they are well defined and functional, sleep spindle analysis is significant for brain research. Identifying the characteristics of sleep spindles may lead to an understanding of the functions of sleep. Furthermore, understanding the sleep spindle generation mechanisms can explain the other rhythmical activity occurring in other brain regions. The detection process of the sleep spindle data of a whole night sleep EEG prepared by an expert would be too time consuming and it may be not objective for some spindle regions. Therefore, an automated detection system would assist the expert. In this thesis, a system for automated detection of sleep spindles in the EEG has been developed and tested on

the recorded data of normal and insomniac subjects. Different methods for the automated detection of sleep spindles in EEG recordings are investigated. Features from the data are extracted by using two different approaches, short time Fourier transform (STFT) and autoregressive (AR) modeling. Multilayer perceptron (MLP) and also support vector machines (SVM) are utilized as classifiers for comparison. The best classification performances of MLP are found to be 97.5% and 93.6% for STFT and AR model features respectively. The best performances of SVM are found to be 97.5% for STFT and 94.4% for AR model. It is demonstrated that the classifiers trained by a healthy subject's EEG could perform well on another healthy subject's EEG but poorly on an insomniac subject's EEG.

Keywords: Sleep Spindles, Multilayer Perceptron, Support Vector Machines, Short Time Fourier Transform, Autoregressive Modeling

ÖZ

UYKU İĞCİKLERİNİN YERİNİN OTOMATİK SAPTANMASI

Görür, Dilan

ELEKTRİK VE ELEKTRONİK MÜHENDİSLİĞİ BÖLÜMÜ

Tez Yöneticisi: Doç. Dr. Nevzat G. Genç

Ortak Tez Yöneticisi: Prof. Dr. Uğur Halıcı

Ocak 2003, 72 sayfa

Uyku iğcikleri, uyku sırasında kaydedilen elektroensefelografi (EEG)'de gözlemlenen ritmik aktivitelere aittir. İyi tanımlanmış ve fonksiyonel oldukları için uyku iğciklerinin analizi beyin araştırmaları açısından önemlidir. Uyku iğciklerinin özelliklerini tanımlamak uykunun işlevi ile ilgili aydınlatıcı bilgiler verecektir. Bütün gece uyku EEG'sindeki uyku iğciklerinin bir uzman tarafından tek tek yerlerinin belirlenmesi çok zaman alıcı olmasının yanı sıra nesnel de olmayacaktır. Bu yüzden, otomatik yer belirleme sistemi uzmana yardımcı olacaktır.

Bu çalışmada EEG'deki uyku iğciklerinin yerlerinin otomatik olarak saptanabilmesi için sağlıklı denekler ve uykusuzluk sorunu olan deneklerin EEG kayıtları kullanılarak bir sistem geliştirilmiştir. Bu amaç için farklı metotlar incelenmiştir.

Öznitelik bulmak için iki ayrı yöntem, kısa zamanlı Fourier dönüşümü (KZFD) ve özyinelemeli (ÖY) modelleme yöntemleri kullanılmıştır. Karşılaştırma amacıyla sınıflandırmada çok katmanlı perseptron (ÇKP) ve destek vektör makinesi (DVM) kullanılmıştır. ÇKP'nin en iyi performansı KZFD ve ÖY modellemeden elde edilen öznitelikler için sırasıyla %97,5 ve %93,6 olarak bulunmuştur. DVM ile elde edilen en iyi başarı oranları ise KZFD için %97,5 ve ÖY modelleme için %94,4 olarak bulunmuştur. Sağlıklı bir denek EEG'si ile eğitilen sınıflandırıcıların başka bir sağlıklı denek EEG'si üzerinde yüksek, uykusuzluk sorunu olan bir denek EEG'si üzerinde ise düşük başarı sağladığı gösterilmiştir.

Anahtar Kelimeler: Uyku içicikleri, Çok Katmanlı Perseptron, Destek Vektör Makinesi, Kısa Zamanlı Fourier Dönüşümü, Özyinelemeli Modelleme

To My Family

ACKNOWLEDGEMENTS

I am grateful to my supervisor Assoc. Prof. Dr. Nevzat Güneri Gençer for his support and understanding through the research. I wish to express sincere appreciation to my co-supervisor Uğur Halıcı for her guidance and invaluable support. I would like to express my gratitude to Prof. Dr. Hamdullah Aydın from GATA Sleep Research Center for cooperation and fruitful ideas. I would like to thank the GATA Sleep Research Center staff for supplying the experimental data and for their help. I wish to thank Dr. Güçlü Ongun for his help. I would also like to thank Prof. Dr. Kemal Leblebicioğlu and Assoc. Prof. Dr. Volkan Atalay for reviewing the thesis.

I thank my brother Anıl Görür for volunteering as one of the subjects and my mother for her patience. I also thank Ömer Akınsoy for his unattainable understanding and support through the research.

Finally, I would like to thank to the members of the METU Computer Vision and Intelligent Systems Research Laboratory for their supporting friendship.

TABLE OF CONTENTS

ABSTRACT	III
ÖZ	V
DEDICATION	VII
ACKNOWLEDGEMENTS	VIII
TABLE OF CONTENTS	IX
LIST OF FIGURES	X
LIST OF TABLES	XII
ABBREVIATIONS	XIV
CHAPTER	
1 INTRODUCTION	1
2 SLEEP	5
2.1 EEG	8
2.2 SLEEP STAGES AND EVALUATION CRITERIA.....	11
2.3 SLEEP SPINDLES	15
2.4 COMPUTERIZED SLEEP ANALYSIS.....	20
3 FEATURE EXTRACTION	25
3.1 STFT	26
3.2 AR MODELING	30
4 CLASSIFICATION	35
4.1 MLP	35
4.2 SVM.....	40
5 RESULTS	46
5.1 DATA SET	46
5.2 FEATURE EXTRACTION	48
5.2.1 <i>STFT</i>	48
5.2.2 <i>AR Modeling</i>	51
5.3 CLASSIFICATION RESULTS	52
5.3.1 <i>MLP</i>	54
5.3.2 <i>SVM</i>	59
6 CONCLUSION	64
REFERENCES	68

LIST OF FIGURES

FIGURE

- 1** Variation of time spent in different sleep stages over years. The amount of NREM sleep decreases with age whereas the amount of REM sleep remains relatively constant [63].7
- 2** Electrode positions according to the 10-20 system. Odd numbered electrodes are positioned over the left hemisphere, whereas even numbered ones are placed over the right hemisphere. Fp=frontopolar, F=frontal, C=central, T=temporal, O=occipital, A=auricular.10
- 3** A polysomnography recording sample (10 *sec* duration) for stage 2 sleep (EEG (C4-A1, O2-A1, C3-A2, O3-A2); right eye EOG (ROC), left eye EOG (LOC); chin, right leg (RLEG) and left leg (LLEG) EMG; ECG). (Recordings taken from the GATA Sleep Research Center).12
- 4** C3-A2 channel of EEG recordings of 5 *sec* for stages awake (W), stage 1 (s1), stage 2 (s2), stage 3 (s3), stage 4 (s4) and REM13
- 5** C4-A1, O2-A1, C3-A2 and O3-A2 channels for demonstrating sleep spindle and K-complex activities. Spindle activity can be easily distinguished visually in the central electrode EEG recordings.16
- 6** Spindle generation network.18
- 7** Examples of some windows used in STFT.29

8	Prediction error filter ($A(z) = 1 + a_1z^{-1} + \dots + a_pz^{-p}$). The output of this filter is approximately white noise if the prediction order is large enough.	31
9	Filter used in AR model obtained by simply inverting the prediction error filter.	31
10	A sample artificial neuron	36
11	The general MLP structure with three layers.	38
12	Two separating hyperplanes with (a) small and (b) larger margins.	40
13	By mapping the nonlinearly separable input data into a higher dimensional feature space, the data can be separated by a linear decision surface.	43
14	Stage 2 EEG and STFT a) original signal for 5 <i>sec</i> interval, b) Hamming window of length 500 <i>msec</i> (M=100) applied at t=1.95 <i>sec</i> , c) windowed signal, d) STFT (2-64 <i>Hz</i>) for a spindle region (the signal shown in (c)) , e) STFT for a non-spindle region, f) STFT (2-64 <i>Hz</i>) for another non-spindle region. The shaded regions denote the spindle frequency range.	50
15	Spectrum of the autocorrelation function (i.e. $R_0 \dots R_p$) of the original signal (+) and the signal obtained by applying white noise to the input of the filter formed by the AR model parameters (•). a) a spindle region b) a non-spindle region c) another non-spindle region.	53
16	The output of MLP for 6 <i>sec</i> stage 2 sleep EEG (C3-A2) for the same subject recorded at two consecutive nights; a)with no medication, b) with hypnotic. (Horizontal axis is time, vertical axis is the output of MLP: 0.5 < spindle < 1, -1 < not spindle < -0.5) The spindle regions are marked by the rectangles.	57

LIST OF TABLES

TABLE

I	The distribution of sleep stages for healthy adult [63]	15
II	Test set results of MLP trained with the STFT features of the insomniac subject.	55
III	Test set results of MLP trained with the AR features of the insomniac subject.	56
IV	Performances of the MLP networks trained using the features obtained by STFT and AR modeling from the healthy subject.	58
V	Performances of the second MLP system on the other healthy subject (351 samples for spindle and 789 samples for non-spindle regions).	59
VI	Performances of the second MLP system on the insomniac subject (875 samples for spindle and 875 samples for non-spindle regions).	59
VII	SVM test set results on STFT features of the insomniac subject. (Gaussian kernel with $C=100$, and $\gamma=1.25$)	60
VIII	SVM test set results on AR features of the insomniac subject (Linear SVM, $C=100$).	61
IX	Performances of the SVMs (Gaussian kernel with $\gamma=0.125$) trained using the 6 fold features obtained from a healthy subject by STFT ($C=500$) and AR modeling ($C=50$).	62

X	Performances of the second SVM system on the other healthy subject (351 samples for spindle and 789 samples for non-spindle regions)	62
XI	Performances of the second SVM system on the insomniac subject (875 samples for spindle and 875 samples for non-spindle regions).	63

ABBREVIATIONS

A	auricular
ANN	artificial neural network
AR	autoregressive
ARMA	autoregressive moving average
C	central
CNS	central nervous system
DFT	discrete Fourier transform
ECG	electrocardiography
EEG	electroencephalography
EMG	electromyography
EOG	electrooculography
EPSP	excitatory postsynaptic potential
F	frontal
FFT	fast Fourier transform
Fp	fontopolar
IPSP	inhibitory postsynaptic potential
LLEG	left leg EMG
LOC	left eye EOG
LTI	linear time invariant
MA	moving average
MLP	multilayer perceptron
NREM	non-rapid eye movement
O	occipital
PE	processing element
PSP	postsynaptic potential
RBF	radial basis function
RE	reticular
REM	rapid eye movement
RLEG	right leg EMG
ROC	right eye EOG
STFT	short time Fourier transform
SVM	support vector machine
T	temporal

CHAPTER I

INTRODUCTION

The brain is a highly complex organ that receives and processes signals from the environment and the body itself and proper actions are taken in response to these signals, enabling man to survive. It also stores information, recalling the relevant information when needed. How the brain works is still relatively poorly understood and there is a wide range of disciplines dealing with different aspects of the problem. The characteristics of the electroencephalography (EEG) waveforms change during sleep and wakefulness, hence brain can be said to be in a different 'state' during sleep than it is during wakefulness. Therefore, sleep studies can improve our insight about the mechanism of the brain. Besides this fact, sleep itself has been a mystery for human beings for ages.

We spend one third of our lives sleeping. Sleep deprivation may cause severe health problems. Sleep deprivation of several days leads to visual illusions, speech slurring, inability to concentrate and memory lapses. Thus, there appears to be a clear biological requirement for sleep. There have been various theories proposed trying to explain the physiological function of sleep [26], but there is no universally accepted theory. In order to understand more about sleep physiology, function and disorders,

extensive sleep-monitoring studies should be carried out on many subjects and over long periods of time. This requires methods for objectively evaluating the sleep process [45].

Scientists focus on the exploration of the macro and micro structure of sleep and also on the physiological activities during sleep. Scientific achievements also depend on the technology. The history of the sleep research is parallel to the progress in the scientific areas such as computer science, mathematics, neuroimaging and neurochemistry. Animal studies are one of the most commonly used empirical models in sleep studies [26, 52]. Another commonly used model is sleep deprivation studies [14, 26, 34, 46]. Applying sleep deprivation of a certain stage of human sleep became possible after the development of staging/scoring of the data. By observing the EEG, the sleep stage of the subject is known, thus it is possible to deprive the subject during a certain stage.

Our knowledge about sleep has increased significantly after the usage of EEG in sleep research. Certain rhythmic activities have been observed in sleep EEG that are characterized according to their frequency, amplitude and duration. How these rhythms are generated is unknown. Regularly occurring patterns such as periodic complexes, alpha rhythm, theta rhythm, sleep spindles and ictal bursts are examples of clinically relevant rhythms. Being one of the well-defined rhythmic activities observed in the sleep EEG, sleep spindles are significant for brain research [43, 50]. Assessment of their distribution over the whole night sleep, their frequency and their relation with the background EEG activity constitutes an important part in sleep studies. Identifying the characteristics of sleep spindles may lead to an understanding of the functions of sleep. Furthermore, understanding the sleep spindle generation

mechanisms can explain the other rhythmical activity occurring in other brain regions.

Having lower amplitude than the background EEG activity, some sleep spindles are hard to be detected by the experts. Thus, the detection process of the sleep spindle data of a whole night sleep EEG prepared by an expert would be too time consuming and it may be not objective. If the studies concerning sleep spindles were carried out using computer-based sleep spindles detection, the subjectivity would be overcome and the process would take much less time. Computer-based sleep spindle detection has several difficulties due to the great variability of spindle morphology and intra-spindle frequency. Therefore, pattern recognition techniques would be a powerful tool for achieving high performances.

This study was done in collaboration with the Sleep Research Center in the Department of Psychiatry of Gülhane Military Medical Academy (GATA). The recordings used were done in the Sleep Research Center and the experts have performed the visual sleep stage scoring. This study attempts to automate the sleep spindle detection. For this purpose, two different classifiers, multilayer perceptron (MLP) and support vector machines (SVM) are utilized in order to have comparative results. The classifiers have been trained using the EEG data labeled by the experts.

For clustering, the sampled EEG recording can be fed directly to the input of the classifier without any preprocessing. However, using appropriate preprocessing steps for extracting features improves the recognition rate and the generalization capability of the classifier.

Sleep spindles are characterized visually by their frequency. In this study, short time Fourier transform (STFT) of the EEG signal are used as features to make use of the

changes of the frequency content of the signal. As an alternative method, autoregressive (AR) modeling, which is a parametric time-domain method, is also used for feature extraction.

The organization of the thesis is as follows: In chapter 2, the sleep process is explained and the sleep spindles are described. In chapter 3, the feature extraction methods STFT and AR modeling and in chapter 4, the classification methods MLP and SVM are explained. In chapter 5, the data set is described and experimental results obtained are given. Finally, chapter 6 concludes the study.

CHAPTER II

SLEEP

Sleep is a behavioral state that differs from wakefulness by a readily reversible loss of reactivity to events in one's environment. This reversibility differentiates sleep from other forms of states of altered consciousness such as coma or a state of anesthesia, which are characterized by unresponsiveness. Various theories have been proposed trying to answer the question why we sleep [59].

The passive theory of sleep suggests that sleep occurs to prevent tiredness or is caused by a lack of sensory stimulation. For ages, sleep used to be considered a passive state of the brain, being opposite of wakefulness. It was thought that excitatory areas of the brainstem and other parts of brain got tired and became inactive, sleep being a result of this inactiveness. There are also active theories that suggest that the brain actively inhibits consciousness [26, 59].

In the last century, our knowledge about sleep has developed significantly. The development of technologies that permit measurement and quantification of brain activity made the macro and micro analysis of brain during sleep and wakefulness possible. By the examination of the central nervous system (CNS), existence of centers that actively cause sleep by inhibiting other parts of brain were observed

[37]. Thus it was concluded that sleep is an actively induced, highly organized brain state, that is, a different state of consciousness.

Sleep studies have gained speed after the development of EEG and its usage in brain research, leading to better understanding and evaluation of sleep. Shortly after the development of the EEG, it was found that brain electrical activity during sleep differed from that of during wakefulness in humans. Hans Berger was the first to study the EEG patterns in relation to sleep. The first classification of sleep based on EEG was developed several years later, dividing the sleep into stages A through E by Loomis and co-workers in 1937 [63]. The criteria differentiating these stages are similar to those in use today. In 1950s, regularly occurring periods of rapid eye movements and other associated phenomena occurring during sleep were recorded in a study of normal subjects. A few years later, the classification of sleep into rapid eye movement (REM) sleep and non rapid eye movement (NREM) sleep was made by Kleitman's group [34]. Aserinsky and Kleitman published data indicating that there are periodic changes on EEG and electrooculography (EOG) channels during sleep in 1953 [5]. They called these changes as REM sleep and defined the two main types of sleep; REM and NREM sleep.

Nowadays, it is well known that REM sleep occurs 3-5 times in every night with 90-120 minute intervals. NREM sleep consists of stages 1, 2, 3 and 4. Stage 3 and 4 are also called deep sleep or delta sleep.

Rechtschaffen and Kales focused on the staging the sleep data and prepared the "sleep stage scoring manual" in 1968 because of the need for standardization of sleep studies [44]. This manual is based basically on Kleitman classification. This classification has persisted until present.

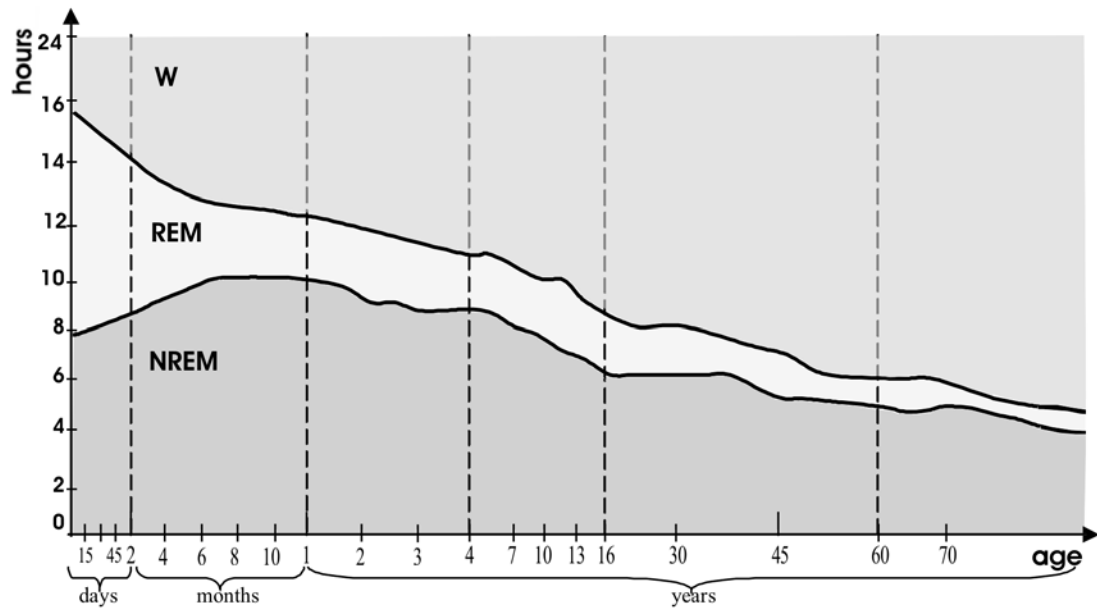


Figure 1 Variation of time spent in different sleep stages over years. The amount of NREM sleep decreases with age whereas the amount of REM sleep remains relatively constant [63].

Constant cycling between NREM and REM, the two basic phases of sleep, forms the sleep pattern, one cycle being within a range of 90 to 120 minutes. The amount of time spent sleeping and the proportion of time in the various states vary with age. The amount of NREM sleep decreases with age whereas the amount of REM sleep remains relatively constant [63] (see Figure 1).

Before the development of EEG devices, sleep was detected and defined solely on the basis of behavioral changes such as specific body posture, maintained behavioral quiescence, elevated arousal threshold and reversibility with stimulation [37]. This

definition is still useful today but electrical recordings are necessary to quantify sleep and observe physiological changes during sleep.

2.1 EEG

The electrical activity of the brain can be recorded by EEG. The frequency of the rhythmic electrical waves recorded varies from 0.5 Hz to 70 Hz and their amplitude varies from $5\ \mu\text{V}$ to $400\ \mu\text{V}$ according to the activity present in the brain. As the activity increases, the EEG frequency gets higher and amplitude gets lower since the synchrony of neurons is disturbed. As sleep deepens, the synchrony of the neurons gets higher, resulting in a high voltage, low frequency EEG. No cerebral activity can be detected from a patient with complete cerebral death.

The measured EEG from a recording site corresponds to the summation of the activity of different parts of the brain. Since electrodes are at the scalp, the activity from deeper nuclear groups such as thalamus cannot be detected due partly to the distance from the recording electrode and partly to the architecture of the thalamic groups that gives rise to closed potential fields [34]. Additionally, it is thought that the action potential time course is too short and the amount of polarized membrane is too small to generate a scalp EEG potential even for the neurons that are close to the skull. Hence EEG is dominated by the activity of the chemical transmitters released at the synapses which cause localized depolarization called as excitatory postsynaptic potential (EPSP) or hyperpolarization called as inhibitory postsynaptic potential (IPSP). Postsynaptic potentials (PSP) of the cortical pyramidal neurons are of longer duration and involve more membrane space.

Since skull is not a good conductor, the instrument to be used for recording EEG should have a high amplification gain. The input impedance of the device should be high. The noise due to both the environment and the body should be eliminated. Both analog and digital EEG devices are commercially available. The resolution of the analog device output is determined by the recording paper speed, which is generally 30 *mm/sec*. The sampling rate of the commercially available digital devices varies between 150 to 300 *Hz*.

The placement of the electrodes is an important point to be considered in EEG recording because the recorded EEG patterns varies with the recording site since the contribution of each activity varies inversely with the distance to the recording electrode. Therefore, it is important that the electrodes are placed at the same points for comparability of the recordings that are taken both from different subjects and from the same subject on different times. The 10-20 system has been generally accepted for standardized electrode placement (see Figure 2). Four anatomical landmarks, the nasion, the inion, and the preauricular points are used to locate the electrode positions. The inter-electrode distances are defined as 10 % or 20 % of the distance between these anatomical landmarks (This is where the system takes its name from.). The electrode positions are named according to the abbreviation of their location on the scalp. The letters Fp, F, C, T, O and A stands for fontopolar, frontal, central, temporal, occipital and auricular regions respectively. Odd numbered electrodes are positioned over the left hemisphere, whereas even numbered ones are placed over the right hemisphere and the electrodes denoted by the letter z are placed over the central regions.

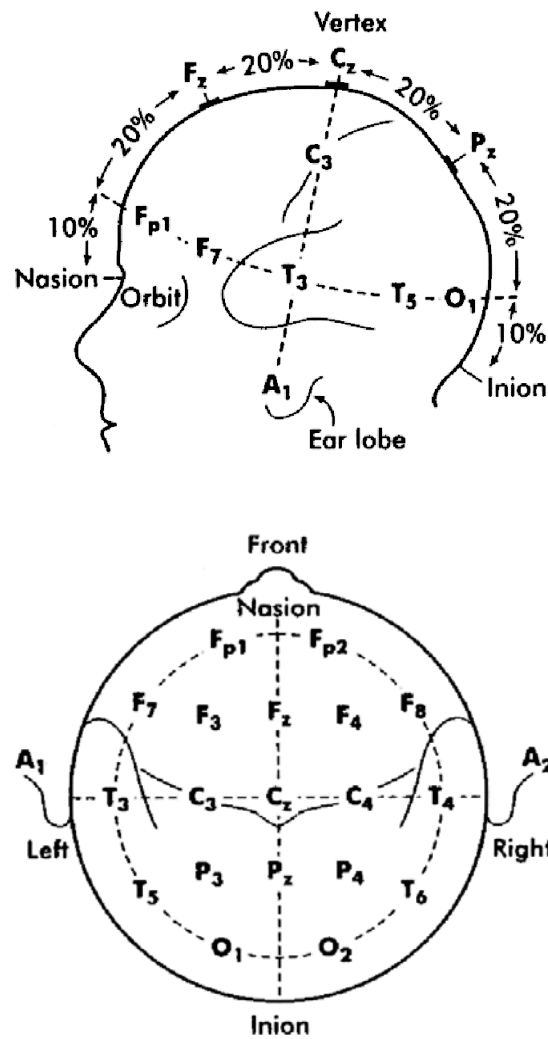


Figure 2 Electrode positions according to the 10-20 system. Odd numbered electrodes are positioned over the left hemisphere, whereas even numbered ones are placed over the right hemisphere. Fp=frontopolar, F=frontal, C=central, T=temporal, O=occipital, A=auricular.

Recordings can be done either monopolarly or bipolarly. In the monopolar (also called as referential) technique, the potentials are measured with respect to a reference electrode. In the 10-20 system, auricular electrodes are used as reference. The potential differences between successive electrodes are measured in bipolar recording technique.

2.2 Sleep Stages and Evaluation Criteria

Electrical recordings are necessary for quantitative sleep analysis and for observing physiological changes during sleep. During sleep, the collective activity of the cortical neurons is monitored by EEG, eye movements by EOG, and muscle activity by electromyography (EMG) by using polysomnograph. These are the physiological parameters necessary for defining sleep stages. The electrocardiography (ECG) data and the respiration data can also be monitored during sleep using polysomnograph if desired. A sample polysomnography recording is shown in Figure 3.

Since the beginning of the EEG recordings, different kinds of oscillations were observed in the background brain electrical activity. EEG spectrum contains some characteristic waveforms that fall primarily within four frequency bands: delta (1–3 *Hz*), theta (4–7 *Hz*), alpha (8–13 *Hz*), and beta (14–20 *Hz*). By examining the EEG recordings, it was shown that sleep is not a passive state of the brain and five stages of sleep were defined.

The earliest detailed classification of sleep into various stages was done by Loomis et al in mid 1930s [30, 63]. The classification of sleep into two main phases by Aserinsky and Kleitman was made in the early 1950s [5].

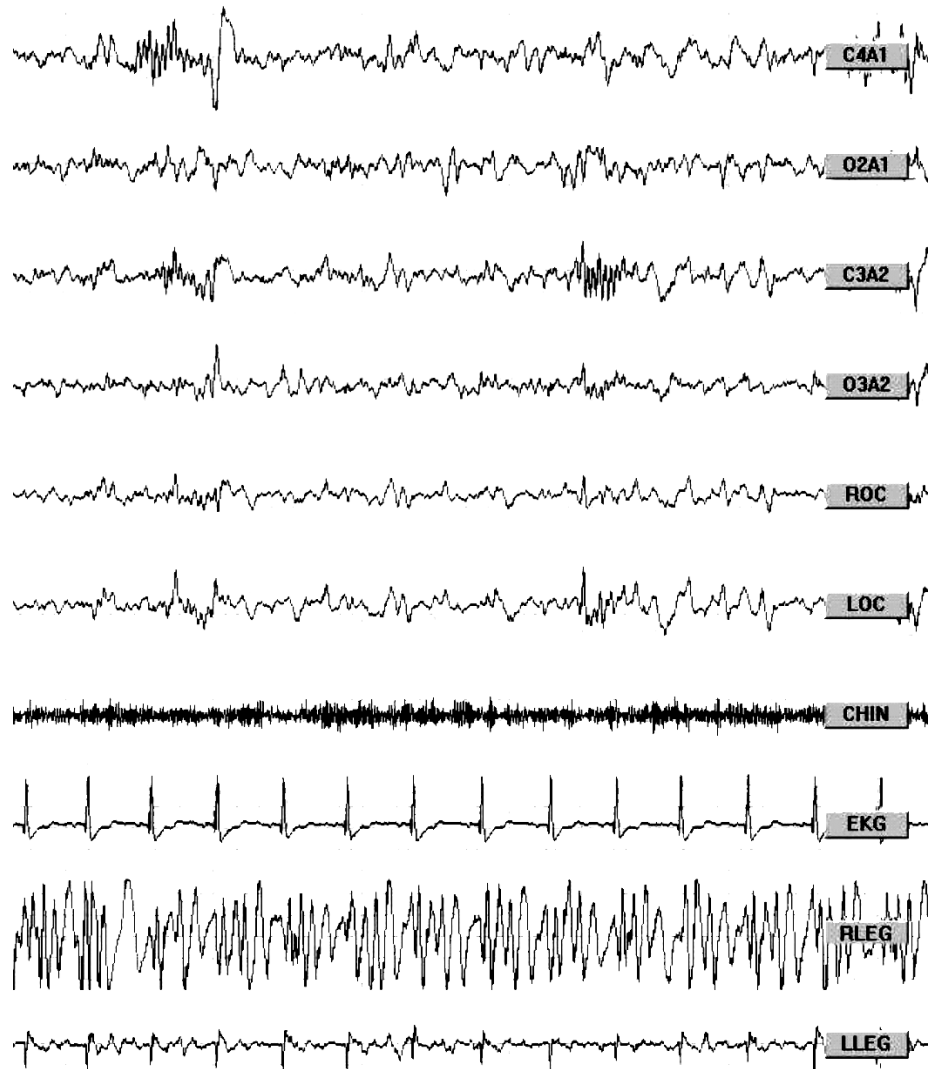


Figure 3 A polysomnography recording sample (10 sec duration) for stage 2 sleep (EEG (C4-A1, O2-A1, C3-A2, O3-A2); right eye EOG (ROC), left eye EOG (LOC); chin, right leg (RLEG) and left leg (LLEG) EMG; ECG). (Recordings taken from the GATA Sleep Research Center)

The two main phases of sleep are the REM and the NREM sleep. REM is the phase of sleep in which the brain seems to be active since high frequency EEG accompanies this stage, thus this stage is also referred to as the paradoxical sleep. NREM is the quiet or restful phase of sleep. Wakefulness, REM sleep and NREM sleep can be said to be different states of consciousness.

NREM is further divided into four stages of progressively deepening sleep (stages 1, 2, 3 and 4) on the basis of EEG changes. Sleep stages can also be identified through EEG signals (see Figure 4).

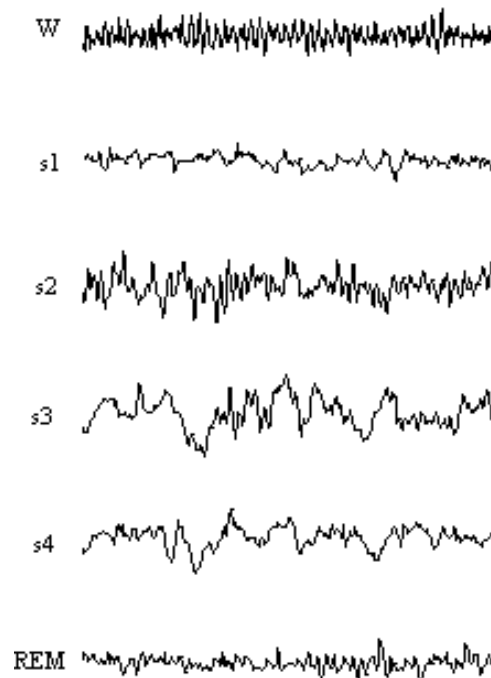


Figure 4 C3-A2 channel of EEG recordings of 5 sec for stages awake (W), stage 1 (s1), stage 2 (s2), stage 3 (s3), stage 4 (s4) and REM

The sleep staging criteria of the manual published by Rechtschaffen and Kales [44] is widely accepted and used for sleep studies. The staging is done on an epoch-by-epoch basis, that is, the polysomnography recordings are divided into 20 or 30 *sec* segments (epochs) and a stage is assigned to each epoch. Below are the staging criteria recapped from this manual.

Wakefulness EEG contains the alpha activity and/or low voltage, mixed frequency activity. Relatively high tonic EMG usually accompanies this stage, and often eye movements and blinks are present in the EOG tracing.

Stage 1 marks the transition from wakefulness to drowsiness. Stage 1 EEG is defined by a relatively low voltage, mixed frequency activity -with a prominence of theta band- and a relative decrease in the muscle tone.

Stage 2 is the predominant sleep stage during a normal night's sleep. In this stage, muscle tone may diminish further. This stage has similar EEG background with superimposed K-complexes and spindles. K-complexes are high-voltage biphasic waves believed to occur as a response to any kind of stimuli. Sleep spindles are high frequency (12-14 *Hz*), relatively low amplitude bursts of sinus like waves with minimum duration of 500 *msec*. These waveforms will be discussed in detail in the next section. This stage EEG may contain up to 20 % delta waves per epoch.

Stages 3 and 4 are characterized by high amplitude (75 μV) delta wave activity. When this activity is greater than the 20% of an epoch (i.e. 20 or 30 *sec* long recording), that epoch is considered as stage 3, when it is more than 50%, as stage 4. Sleep spindles and K-complexes become rare in stage 3 and disappear in stage 4. The muscle tone decreases further in these stages.

In the REM stage, as the name indicates, rapid eye movements are seen, EEG is characterized by low amplitude and mixed frequency, and muscles except for those of the eye and the respiratory system loose their tonus.

The amount of time spent in each sleep stage varies with age as mentioned earlier (depicted in Figure 1) but the distribution of the sleep stages is similar for healthy subjects of the same age. The distribution of the sleep stages of a healthy adult is presented in Table I.

Table I The distribution of sleep stages for healthy adult [63]

Stage 1	5-10 %
Stage 2	45-60 %
Stages 3 & 4	20-25 %
REM	20-30 %

2.3 Sleep Spindles

Sleep spindles, first described in human EEG by Loomis et al (1935) are transient waveforms of frequency around 13 *Hz* observed at the cortical pyramidal neurons driven by the thalamo-cortical (from thalamus to cortex) oscillations that are active during sleep [13]. They are present during NREM sleep, being most prominent during stage 2. Their presence should not be mentioned unless the activity is of at

least 500 *msec* duration [44]. They are most readily recorded from the central and the centroparietal brain regions. An EEG recording of the C4-A1 and C3-A2 channels containing sleep spindle activity is depicted in Figure 5.

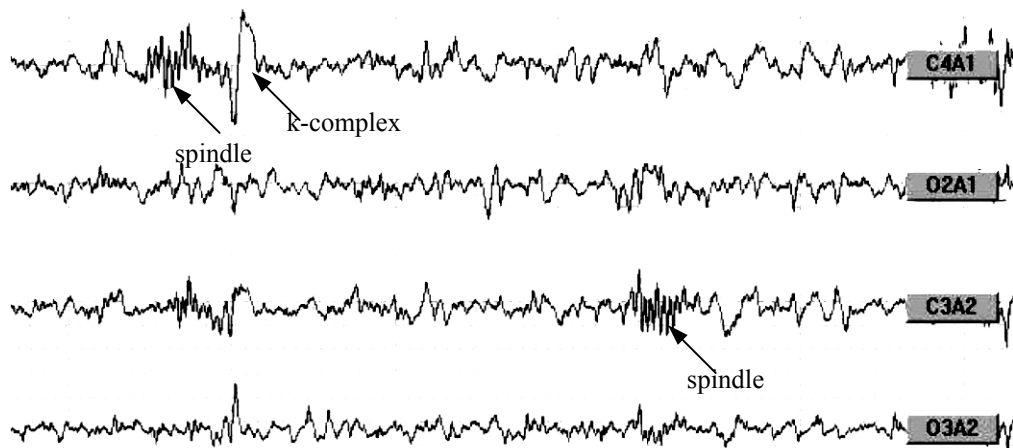


Figure 5 C4-A1, O2-A1, C3-A2 and O3-A2 channels for demonstrating sleep spindle and K-complex activities. Spindle activity can be easily distinguished visually in the central electrode EEG recordings.

Spindle activity has been studied in a variety of conditions. It increases in association with motor disorders, but decreases in cases of cerebral tumors or following certain cortical surgical procedures.

The development of the CNS and sleep pattern has correspondences. Rudimentary spindles can be detected in the EEG of full-term (i.e., not prematurely born) infants at 4 weeks of age. The duration of the activity gets longer and its amplitude increases in time [22]. The longest spindle formation is observed between 1.5-3 months [35].

These observations suggest that spindles become fully developed within 3 months. The rapid development of the spindle patterns within the first 3 months of infancy possibly reflects the developmental changes in the thalamo-cortical structures and maturation of the physiological system that produces spindles [35]. Spindles reach a maximum density between 4-6 months and their incidence decrease until the fifth year of life.

Prematurely born infants have reduced spindle activity initially but this is compensated in a couple of months [35].

The above observations cause the scientists to reason that there is a close relation between the sleep spindle structure and brain maturation.

Spindle activity increases over consecutive sleep cycles. They are present in sleep throughout life, their density decreasing with age.

The frequency of the spindle activity increases with age [36, 43]. Sleep spindles are observed to occur both as a spontaneous activity of the thalamus and before or after the appearance of the K-complexes, which are believed to occur in response to any kind of stimuli. Therefore, the second kind of sleep spindle activity is believed to have a sleep-preserving role by attenuating the potentially arousing stimuli.

Thalamo-cortical interaction is one of the main circuits for wakefulness and sleep. During wakefulness, the circuit receives input from and gives output to the related areas. During the transition from wakefulness to sleep, the circuit becomes inactive. It could be claimed that this inactivation makes the EEG waveforms more unified. As sleep deepens, main EEG wave can be easily observed. Spindle is one of these waveforms.

Spindling appears to be a network-generated oscillation of the thalamo-cortical - thalamic reticular (RE) nucleus - thalamic neurons [16]. The RE nucleus receives input from the rostral brain stem and the basal forebrain, and projects mainly to the dorsal thalamus, with minor output to the rostral brain stem [32] (see Figure 6).

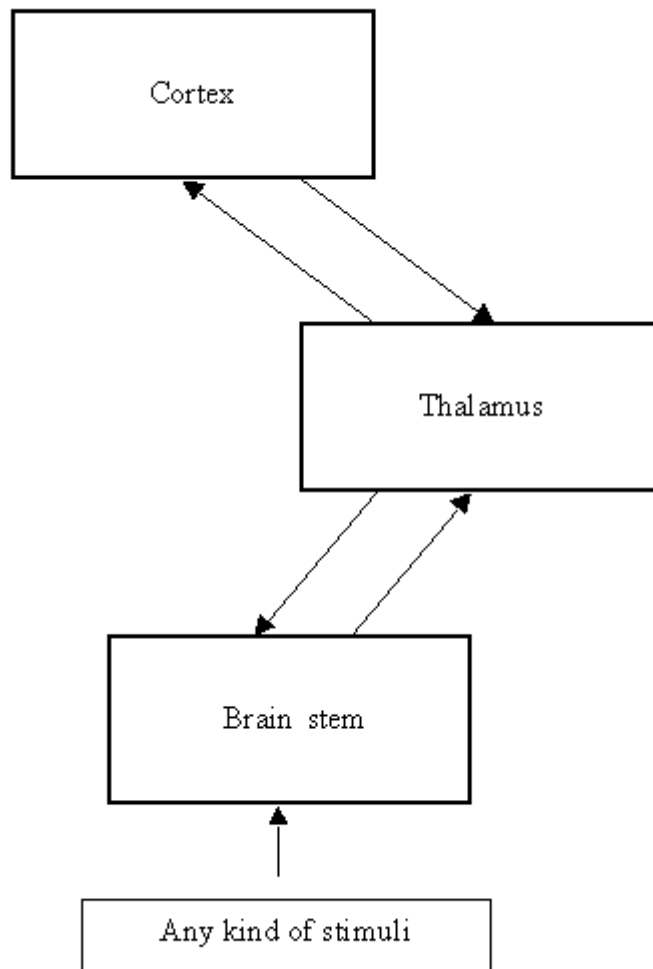


Figure 6 Spindle generation network

The dorsal thalamic nuclei project to the cortex and both structures resonate with the spindle frequency and reinforce the oscillation. The pacemaker driving sleep spindles is thought to reside in the RE cells. The RE cells generate a spontaneous rhythm and drive other thalamic cells to produce spindles [51, 52].

It is thought that the thalamic neurons may have spontaneous rhythmic activity and event related activities [6]. The spontaneous activity may show one of the basic functions of the neurons. Having spontaneous and aperiodic oscillations may indicate that these structures play a role as a pacemaker. If this is true, brain shows two types of oscillations. One of them is spontaneous, the other one is event related.

Sleep spindles are the example of these two types of oscillations. For this reason, spindle form is worth evaluating and analyzing in terms of frequency and amplitude.

Spindles, as an event related phenomena, are easily observed as a part of k-complexes. Some spindles take place just before or just after k-complexes. K-complexes are considered as a cortical response to stimuli. In the light of this approach, spindles are considered as a thalamocortical interaction and as a regulation/ restoration phenomenon.

The study of EEG can explain the mechanisms of sleep and wakefulness and thus can shed light on the neurophysiological basis of consciousness. Sleep spindle is a characteristic transient waveform in sleep EEG. Being easy to recognize as compared to many other waveforms, it is of great significance for sleep EEG analysis. It is useful for classification of NREM sleep, particularly stage 2, and to evaluate the degree of arousal [37]. The amount and distribution of sleep spindles and their relation to other rhythms of EEG can be used to describe the morphology of the sleep EEG [14, 15, 58]. The density and frequency of the spindles change with age. This

can be used to evaluate the degree of brain maturity. Neurological disorders may cause changes in the characteristics of sleep spindles [56]. Thus, the assessment of sleep spindles is of potential interest for evaluation of neurological disorders as well. Some drugs are known to influence the sleep spindles. The effects of chemicals on CNS can be investigated by observing the changes of sleep spindle characteristics.

It is assumed that regardless of the frequency of discharge, underlying mechanisms are similar. Sleep spindles have been particularly well examined owing to their striking rhythmicity and much is known about the underlying circuitry of spindle generation as compared to other brain rhythms [65]. These mechanisms can be generalized to other types of rhythmical activity arising from different brain regions; however, this should be done cautiously as such mechanisms may be dissimilar.

2.4 Computerized Sleep Analysis

Quantitative analysis of the structure and the dynamics of sleep was realized with the development of EEG and the technology that made the continuous recording over long periods possible. Computerized analysis of sleep leads to a better understanding of the dynamics and the time course of the EEG waveforms.

Computerized sleep studies include automated sleep stage scoring [1, 29, 38, 45], artifact detection [48], investigation of the evolution of the spectral power in the NREM and the REM episodes [33, 46, 54], classification of the EEG of subjects with different CNS disorders [27], analysis of the effects of drugs on EEG, source localization [53, 57], analysis of the sleep-wake transition [37] and detection and analysis of transient waveforms [4, 9, 12, 19, 23, 24, 25].

Sleep staging is a very important process in sleep studies. The distribution and length of the sleep stages over night gives information about the quality of sleep. Besides, sleep deprivation is one of the most commonly used empirical methods in sleep studies. By knowing the sleep stage the subject is going through, deprivation of a certain stage may be applied easily. Having such an important place in sleep studies, the need for automated sleep staging draws much attention. There are methods proposed which implements sleep staging with or without depending on the previously defined rules.

Kohonen self organizing network is used to distinguish between different sleep stages without the use of predefined rules or assumptions in [45]. The features are extracted using Kalman filter of order 10. As the result of the study, eight types of clusters were found.

Automatic sleep stage classification which uses feedforward backpropagation network for classifying the features extracted by using wavelet transform is implemented with 70 to 80% agreement with the human expert in [39].

There are some systems proposed that make use of both the supervised and unsupervised learning. Initially, clusters of the data by the k-means clustering algorithm are formed in [1]. Then, sample epochs are presented to the user for classifying these samples according to any classification standard. The method then learns from these samples to complete the classification, resulting in an overall concurrence of 80.6% with manual scoring done according to the Rechtschaffen and Kales standard [44]. The feature vectors used in this method are formed for the segments of the EEG using various features of the segments including the amplitude, dominant rhythm (evaluated using a second order AR model), the frequency

weighted energy (defined by the nonlinear energy operator), the ratio of power in the sigma band (to assess the presence of sleep spindles), the ratio of the power in the alpha band to the combined power in the delta and theta bands, the ratio of the power in the theta band to the combined power in the delta and alpha bands and the presence of the eye movements.

Studies concerning the sleep spindles include determination of their topographical distribution in sleep EEG [15, 54], localization in brain [53], investigation of variation of the activity over consecutive NREM sleep episodes [17], analysis of the effects of various drugs and age on sleep spindle formation [36], analysis of sleep spindles dynamics [3, 9, 20, 65, 66], analysis of their generation mechanisms and investigation of the sleep spindle characteristics in presence of CNS disorders [11].

Time frequency analysis methods, time domain methods and filter methods are used for extracting features in computerized sleep spindles analysis studies. For classification and detection purposes statistical measures, artificial neural networks and kernel based methods have been used.

It is known that sleep spindle characteristics change with age. Sleep spindle characteristics in healthy subjects of different age groups is assessed in [36] by non-parametric Kruskal-Wallis analyses of variance. The results of [36] show that there is a progressive decrease in spindle number, density and duration and a progressive increase in the intra-spindle frequency with age.

The variation of slow-wave activity and sleep spindles over consecutive non-REM sleep episodes with relation to prior sleep are investigated in [17] using both spectral analysis by fast Fourier transform (FFT) and a transient pattern recognition software.

Higher order statistical measures both in time and frequency domains are used to investigate the sleep spindle activity related with stage 2 sleep in [3]. The time domain techniques combining the use of second and third order correlations are used to investigate the non-stationary behavior of the spindles while the frequency domain method is used to investigate frequency interactions which might be due to the nonlinearities observed in the EEG.

FFT of 2 *sec* epochs are used to investigate the sleep spindle asymmetry in patients with idiopathic epilepsy, cryptogenic epilepsy, and symptomatic partial epilepsy in [11].

Automated detection of sleep spindles is significant in sleep spindle studies since there are hundreds of spindle occurrences in a night's sleep and each has to be detected in order to assess the change in characteristics over whole sleep. Therefore, there are many studies seeking to optimize the automated spindle detection. Matching pursuit is used to parameterize the EEG and the presence of the spindle is decided based on the frequency, time width and amplitude criteria in [65, 66]. The agreement between the automatic method and the experts increased up to 90% with increasing amplitude threshold value in [66]. In [4], the Discrete Wavelet transform is presented as an alternative method to capture the spindle activity. Detection of sleep spindles by using 3rd order type 1 bandpass Chebycheff filter is investigated in [64]. Wavelet transform together with Teager Energy operator has been used to determine the presence of spindles in [21]. No performance percentage was supplied in these studies.

Besides software detection systems, hardware systems have also been implemented for spindle detection. In 1980, Campbell et al. reported up to 72% true positives by

using phase-locked loop and complex demodulation circuitry [8]. The performance of the 'spindicator' which was initially 73.5% could be raised up to 98.4% when the discrepancies between the two individual scorers were resolved by mutual consensus [42].

CHAPTER III

FEATURE EXTRACTION

Clustering can be applied directly on time-segments of the sampled raw data without any preprocessing. However, using appropriate preprocessing steps for extracting features improves the recognition rate and the generalization capability of the classifier. Therefore, the feature vectors should be extracted from the sleep EEG recordings.

The spectral information of the EEG signal can be used for this purpose since the sleep spindles are differentiated in the EEG activity by their frequency characteristics. Fourier transform is a powerful tool to study the frequency content of signals but has the drawback that it does not provide any localization in time [62]. To obtain localization in time, short time Fourier transform (STFT) is used as one of the feature extraction methods in this study.

The stochastic properties of the EEG signal can also be used for feature extraction. Signal modeling is the design of filters to represent the random processes that have some desired power density spectrum or correlation function. In this study, the autoregressive (AR) model is formed using the second order characteristics, namely,

the correlation function of the EEG signal, as an alternative feature extraction method.

3.1 STFT

Fourier transform is a mathematical tool that is used to expand the signals into a spectrum of sinusoidal components, coefficients of the transform revealing the contribution of each sinusoidal component. A continuous time signal $x(t)$ and its Fourier transform $X(\omega)$ are related by the set of equations (1) for any $x(t)$ for which the integral (1.a) converges.

$$X(\omega) = \int_{-\infty}^{\infty} x(t)e^{-j\omega t} dt \quad (1.a)$$

$$x(t) = \int_{-\infty}^{\infty} X(\omega)e^{j\omega t} d\omega \quad (1.b)$$

The Fourier transform of a sequence (discrete-time Fourier transform) and its inverse transform are represented by the following set of equations

$$X(\omega) = \sum_{-\infty}^{\infty} x[n]e^{-j\omega n} \quad (2.a)$$

$$x[n] = \frac{1}{2\pi} \int_{-\pi}^{\pi} X(\omega)e^{j\omega n} d\omega \quad (2.b)$$

In the above equations, the time variable n is discrete whereas the frequency variable ω is continuous, ranging over an interval of length 2π .

Discrete Fourier transform (DFT) is an approximation of the Fourier transform that can be calculated from a finite number of discrete time samples of a signal and that

produces a finite set of discrete frequency spectrum values for digital processing. Considering the finite-length sequence $x[n]$ of length N , the DFT and the inverse DFT are defined as;

$$X[k] = \sum_{n=0}^{N-1} x[n] e^{-j2\pi kn/N} \quad (3.a)$$

$$x[n] = \frac{1}{N} \sum_{k=0}^{N-1} X[k] e^{j2\pi kn/N} \quad (3.b)$$

Fourier transform assumes that the amplitude, frequency and phase properties of the signal under consideration do not change with time. However, the properties of the signals generally change with time in practice, therefore time localization is necessary while analyzing the signal. When dealing with such signals, Fourier transform is not sufficient since it does not provide any localization in time and a tool that can express the signal in both time and frequency domains is required. Therefore, the concept of STFT, also called windowed Fourier or Gabor transform was introduced, which is the localization of the Fourier transform using an appropriate window function centered on a location of interest [38]. STFT is an expansion along two parameters, frequency and time shift. It consists of a separate Fourier transform for each instant in time. In particular, for each instant, the Fourier transform of the signal in the neighborhood of that instant is associated. The STFT of a sequence $x[n]$ is defined as

$$X[n, \lambda] = \sum_{m=-\infty}^{\infty} x[n+m] w[m] e^{-j\lambda m} \quad (4)$$

where $w[m]$ is a window sequence. n denotes the discrete variable of time whereas λ denotes the continuous variable of frequency and to make clear this notation, different parentheses have been used for denoting the continuous and the discrete variables.

For digital processing, the discrete-time STFT (which is continuous in frequency) is sampled:

$$X[n, k] = X[n, \lambda] \Big|_{\lambda=2\pi k / N} \quad (5)$$

There is no admissibility constraint on the window function, except for it to have finite energy. The STFT of a signal is the Fourier transform of the short-time sections of that signal, obtained by multiplying the signal with the window function. The Fourier transform of the product of two sequences is given by the convolution of their respective Fourier transforms. Thus, for an accurate reproduction of the properties of the original signal around the desired time instant, the Fourier transform of the window function should be close to an impulse with respect to the Fourier transform of the original signal. A rectangular window would have poor frequency localization therefore smoother windows are preferred. Triangular window, Hanning window, Gaussian window and Hamming window are some smoother windows designed for data analysis (see Figure 7) [38].

A second issue in analysis window selection is the compromise required between a long window for frequency resolution and a short window for not allowing the temporal properties of the signal to vary appreciably.

In this study, the Hamming window of length 100 samples (500 msec) is used:

$$w[n] = \begin{cases} 0.54 - 0.54 \cos(2\pi n / M), & 0 < n < M \\ 0, & \text{otherwise} \end{cases} \quad (6)$$

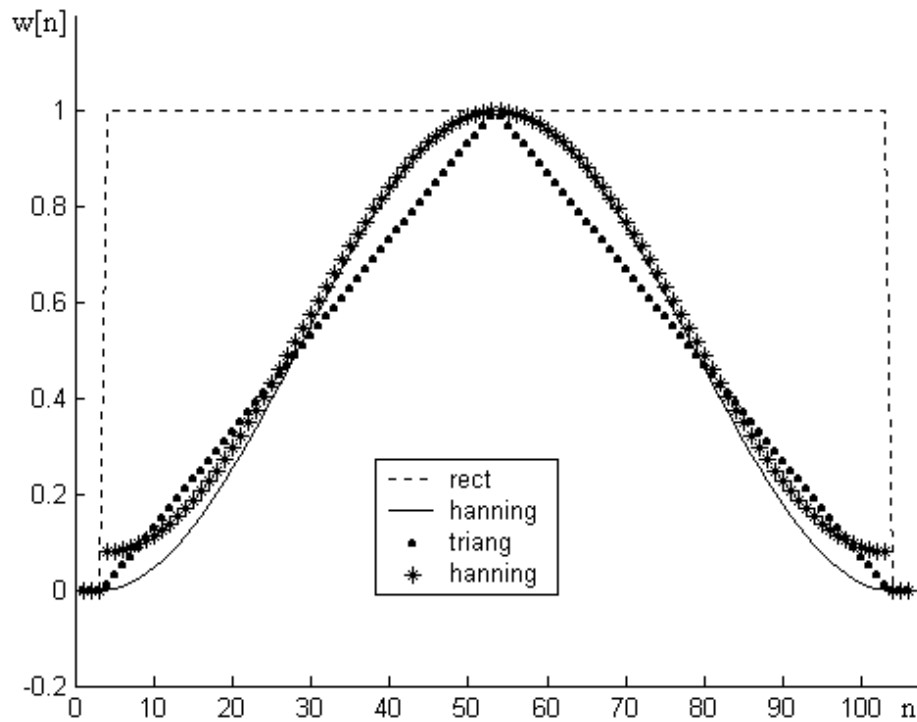


Figure 7 Examples of some windows used in STFT

The STFT of a signal at a particular time instant is computed over the signal by multiplying the signal by the window function centered on the time of interest as explained above. The whole time domain is covered by shifting the window function along the signal with steps usually shorter than the window length. Thus, the time resolution also depends on the size of shifts taken in time.

The same window function is used for obtaining the STFT of the whole signal. Therefore, the time and frequency localization of the STFT is fixed for all time and frequency scales.

3.2 AR Modeling

Random processes can be described by means of a parametric model [31]. Parametric modeling tries to fit a mathematical model to the sampled signal, thus reduces a complicated process with many variables to a simpler one with a smaller number of parameters. There are three basic types of linear models; the all-pole model, the all-zero model and the pole-zero model which are also referred to as the autoregressive (AR) model, the moving average (MA) model and the autoregressive moving average (ARMA) model, respectively. AR model is the one most frequently used among the three due to its relative easy design.

Linear combination of the samples of a signal can be used to predict the future value of the signal, known as linear prediction. In mathematical terms, given a signal $x[n]$, $n=0, 1, 2, \dots, N-1$, we want to predict the value of $x[N]$.

$$x_p[n] = \sum_{i=1}^p -a_i x[n-i] \quad (7)$$

where p is the prediction order indicating that only the p previous values of the sequence are used in the estimation and a_i are the prediction coefficients. Defining $a_0 \equiv 1$, the prediction error can be written as:

$$e[n] = x[n] - x_p[n] = \sum_{i=0}^p a_i x[n-i]. \quad (8)$$

The output of the prediction error filter (Figure 8) is approximately a white noise process if the prediction order is large enough [55].

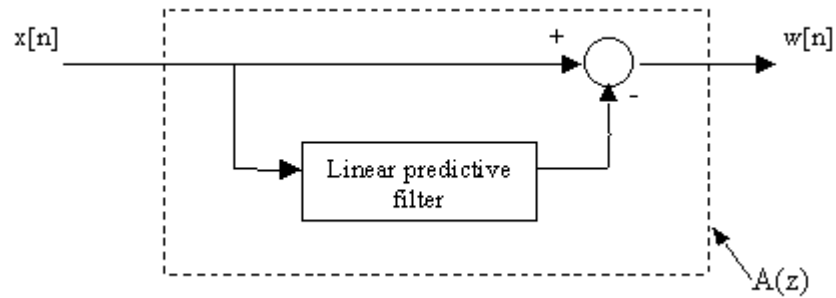


Figure 8 Prediction error filter ($A(z) = 1 + a_1z^{-1} + \dots + a_pz^{-p}$). The output of this filter is approximately white noise if the prediction order is large enough.

If the prediction error filter is inverted and is driven with a white noise sequence (Figure 9), this system would then produce a random sequence with the same statistical characteristics (such as autocorrelation or covariance functions) as those of the original sequence, thus representing a model for the process [55].

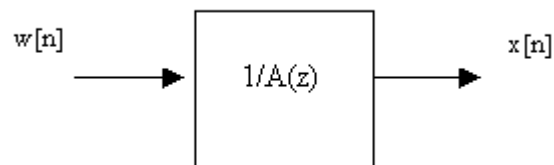


Figure 9 Filter used in AR model obtained by simply inverting the prediction error filter.

The filter of the model has the transfer function $H(z) = 1/A(z)$, that is, it is a filter with all of its zeros at the origin in the z -plane. Therefore, the model is called an all-pole model. The output of such a filter for white noise input is an autoregressive process, that is, the original sequence $x[n]$ is expressed as the linear combinations of the past observations weighted with the coefficients a_1, a_2, \dots, a_p , where p is the model order.

$$x[n] = -\sum_{i=1}^p a_i x[n-i] + e[n] \quad (9)$$

For this reason, this model is also referred to as the AR model.

Several methods exist to estimate the autoregressive parameters, such as least squares, Yule-Walker and Burg's method [41]. These estimation techniques lead to approximately the same parameter estimates [55]. In this study, the most widely used technique, Yule-Walker Equations are used for solving for the coefficients a_1 to a_p :

$$\begin{bmatrix} R_0 & R_1 & R_2 & \cdots & R_p \\ R_1 & R_0 & R_1 & \cdots & R_{p-1} \\ R_2 & R_1 & R_0 & & R_{p-2} \\ \vdots & \vdots & \vdots & \ddots & \vdots \\ R_p & R_{p-1} & R_{p-2} & \cdots & R_0 \end{bmatrix} \begin{bmatrix} 1 \\ a_1 \\ a_2 \\ \vdots \\ a_p \end{bmatrix} = \begin{bmatrix} E \\ 0 \\ 0 \\ \vdots \\ 0 \end{bmatrix} \quad (10)$$

where E is the sum of the squared errors and R_i denotes the i^{th} term of the correlation function. The coefficients a_1 to a_p and the error term E can be obtained by solving the $P+1$ equations with $P+1$ unknowns represented by the above matrix equation.

The model is formed using the correlation function of the EEG signal. Since the correlation function R_i of EEG is not known a priori, it needs to be estimated from

the given observation of the process. There are two common data-oriented methods, namely, the autocorrelation and the covariance methods. In this study, the correlation function is estimated using autocorrelation method;

$$R_{|i-j|} = \sum_{n=1}^N x[n-i]x[n-j], \quad \text{for} \quad \begin{array}{l} 0 \leq i \leq p \\ 0 \leq j \leq p \end{array} \quad (11)$$

The model parameters (i.e., $a_1 \dots a_p$) are chosen so as to give the best fit to the data sequence, therefore the model requires the signal under consideration to be stationary. Although many signals are nonstationary and cannot be modeled with just one linear time invariant (LTI) system, it is often possible to model small sections of a signal and then account for nonstationarity by allowing the parameters of the model to change from section to section. The stationarity requirement is not satisfied in the case of EEG, but EEG can as well be divided into sufficiently short quasi-stationary segments. In this study, segments of 500 *msec* duration are used. This is a proper choice since the necessity of being not less than 500 *msec* duration is also in the definition of sleep spindles [44].

The choice of the model order is an important issue in the estimation of parametric models. If the data is in fact a finite order autoregressive process, then the theoretical prediction error variance becomes constant when the model order is reached. However, in practice the estimated quantities might not converge at all. Thus, the optimum model order is best estimated by maximizing the goodness of fit, that is, minimizing E in equation (10), and limiting the complexity of the model. This is why minimizing the error would not be enough and there needs to be a factor for penalizing the higher order models. There are various criteria proposed for choosing

the best model order such as Akaike's information-theoretic criteria, Parzen's criterion autoregressive transfer, Akaike's final prediction error and Schwartz and Rissanen's minimum description length [55, 61].

When AR modeling is used for extracting features from EEG, the EEG is first segmented into short quasi-stationary segments. A different AR model is calculated for each segment and the model parameters are used as the feature vectors for classifying the segments.

Different criteria result in different best model order estimates. Besides, the best order estimate varies for different EEG segments even if the same criterion is used. The important point in feature extraction is being able to represent data belonging to different classes with separable feature vectors. AR modeling can also be used for spectral estimation [31] where model order selection is more critical, but this is out of the scope of this work.

AR modeling is used as one of the feature extraction methods in this study. Thus, we have not used any of the criteria mentioned above for choosing the model order. Instead, different feature sets were formed using parameters of different order models. A separate classifier was trained with each feature set to find out which order model gave the best classification performance. The best classification performance was obtained using the 16th order model.

CHAPTER IV

CLASSIFICATION

Two different classifiers, MLP (Multilayer Perceptron) and SVM (Support Vector Machines), have been used for the classification of the EEG recordings into spindle and non-spindle regions. For training and testing of both classifiers, two different feature vector sets obtained from STFT and AR modeling have been used.

4.1 MLP

In biological neurons, the signal is transmitted from one neuron to another through the synapses. Transmitter substances are released increasing or decreasing the electrical potential of the receiving neuron, the process being called as excitation and inhibition respectively. If the potential of the neuron reaches a threshold value, the neuron fires. The inhibition and excitation of synapses can be enhanced by the activities of the neurons. This plasticity of the synapses is believed to be the neuronal mechanism of learning and memory functions of the brain.

The artificial neuron is inspired from the biological neuron. A typical processing element (PE) is depicted in Figure 10.

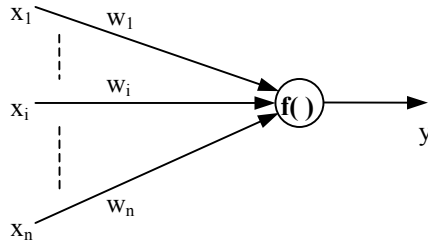


Figure 10 A sample artificial neuron

x_i are the inputs and y is the output of the PE. An adjustable value called weight or connection strength is associated with each input connection. This is a direct imitation of synaptic plasticity. The operation of a single unit can be expressed as

$$y_j = f\left(\sum_{i=1}^n x_i w_{ij} + \theta_j\right) \quad (12)$$

where w_{ij} is the weight of the connection from unit i to unit j , θ_j is the threshold of the unit and $f(\cdot)$ is called the activation function.

Most commonly used activation functions are the linear, ramp, step and sigmoid functions [18].

$$f(x) = \alpha x \quad \text{linear}$$

$$f(x) = \begin{cases} S & , x > S \\ x & , |x| \leq S \\ -S & , ow \end{cases} \quad \text{ramp}$$

$$f(x) = \begin{cases} S & , x > 0 \\ -S & , ow \end{cases} \quad \text{step}$$

$$f(x) = \frac{1 - e^{-x}}{1 + e^{-x}} \quad \text{sigmoid}$$

(13)

Similar to the biological neural networks, the PEs (artificial neurons) are used as the building blocks for an artificial neural network (ANN). An ANN is an adaptive, most often non-linear system that learns to perform a mapping of input to output from data. Different ANN architectures are formed using the PEs with different connection topologies. Besides the architecture, the learning algorithm is also an important feature distinguishing different kinds of networks. Learning is a process by which the free parameters (i.e., synaptic weights and bias levels) of a neural network are adapted through a continuing process of stimulation by the environment in which the network is surrounded [2]. The ANN is trained by a systematic procedure to optimize a performance criterion or to follow some implicit internal constraint, which is commonly referred to as the learning rule. The type of learning determines the manner in which the parameters are updated. Learning machines can be mainly classified as supervised and unsupervised.

In supervised learning, the set of training data made up of input-output examples are labeled by a supervisor prior to training. Given the training sample, the requirement is to compute the free parameters of the neural network so that the actual output due to the input is close enough to the obtained output of the neural network in a statistical sense.

In unsupervised learning, there is no supervisor. The goal is to separate the data set into clusters. The system forms clusters of the given examples by updating the free parameters according to the learning rule. Therefore, different clustering algorithms may lead to different clusters for the same set of patterns.

After the training phase, the ANN parameters are fixed and the system is set out to solve the problem at hand (testing phase).

MLP, a neural network structure which uses supervised training is used in this study. MLP is a layered arrangement of PEs in which the output of each layer is connected to the input of the next layer. An MLP has an input layer of source nodes, an output layer of neurons, and one or more layers of hidden neurons, which are so called because they do not have direct connection with the input or output end of the network structure.

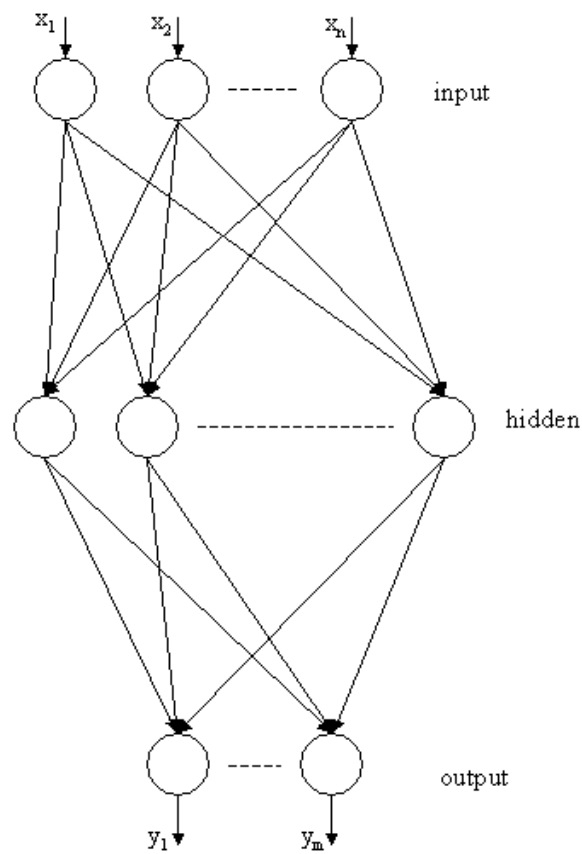


Figure 11 The general MLP structure with three layers

Each connection between the neurons is weighted by a scalar, called a connection weight which is adapted during learning. The MLP structure is depicted in Figure (11).

The backpropagation of error algorithm is the one most widely used for training MLP [47]. In the backpropagation algorithm, the output error is propagated backward through the connections to the previous layers.

There are two phases in the training process, feedforward and backpropagation. In the feedforward phase, each input sample is presented to the input layer and the output of the network is computed. In the backpropagation phase, the obtained output value is compared with the desired output value and the error is propagated backward through each layer to the input layer.

The stop criterion is a fundamental aspect of training. The simple idea of capping the number of iterations or of letting the system train until a predetermined error value is reached are not recommended. The reason is that we want the ANN to perform well in the test set data, i.e., we want the system to perform well in the data that it never saw before (good generalization). The error in the training set tends to decrease with iteration when the ANN has enough degrees of freedom to represent the input/output map. However, the system might be remembering the training patterns (overfitting) instead of finding the underlying mapping rule. This is called overlearning. To avoid overlearning, the performance in a validation set, i.e., a set of input data that the system never saw in the training phase, must be checked regularly during training. The training should be stopped when the performance in the validation set starts to decrease, despite the fact that the performance in the training set continues to

increase. This method is called cross-validation. The validation set should be distinct from the training or the testing sets.

The MATLAB Neural Network toolbox is used for forming the MLP networks in this study.

4.2 SVM

Support vector machine (SVM) is a classification and regression method drawing much attention recently. It can be seen as an alternative technique for polynomial, radial basis function and multilayer perceptron classifiers [28]. It combines methods of statistics, machine learning and neural networks. One of the most important features of SVM is the use of kernels for solving nonlinear problems. That is, the concept of transforming linear algorithms into nonlinear ones via mapping into a different feature space [49].

In a two-class classification problem, the goal is to separate the classes by a function which is induced from the training examples and that generalizes well.

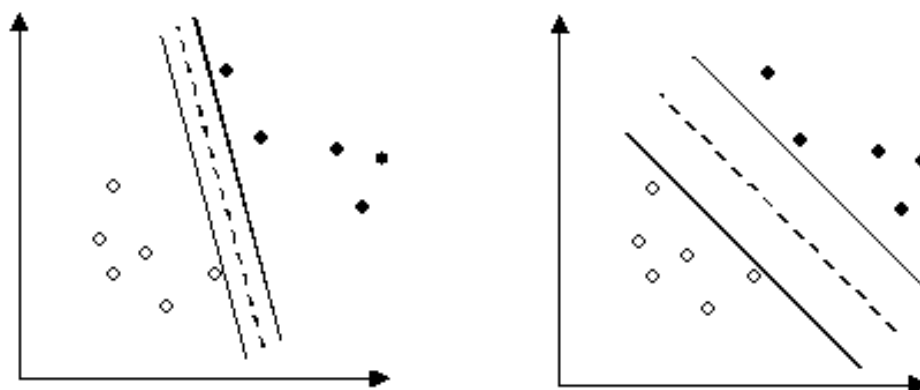


Figure 12 Two separating hyperplanes with (a) small and (b) larger margins

The main idea of SVM is to separate the classes with a surface that maximizes the margin, that is, that has maximum distance between it and the nearest data points of each class, so as to generalize better than other possible boundaries. See Figure 12 for an illustration of two possible hyperplanes that can be used in a classification problem.

Given a set of linearly separable samples (\mathbf{x}_i, y_i) , where \mathbf{x}_i are the training inputs and y_i are the corresponding observations where $\mathbf{x}_i \in \mathfrak{R}^N$, $y_i \in \{-1,1\}$, the solution of the classification problem could be found by solving the following optimization problem:

$$\begin{aligned}
 & \min \\
 & \quad \Phi(\mathbf{w}) = \frac{1}{2} \|\mathbf{w}\|^2 \\
 & \text{s.t.} \\
 & \quad y_i(\mathbf{w} \cdot \mathbf{x}_i + b) \geq 1 \quad i = 1 \dots l
 \end{aligned} \tag{14}$$

where $\frac{2}{\|\mathbf{w}\|^2}$ determines the width of the margin. The solution of the above problem can be found by the saddle point of the Lagrange functional constructed from both the objective function and the corresponding constraints:

$$L(\mathbf{w}, b, \Lambda) = \frac{1}{2} \|\mathbf{w}\|^2 - \sum_{i=1}^l \lambda_i [y_i(\mathbf{w} \cdot \mathbf{x}_i + b) - 1] \tag{15}$$

where Λ is the vector of nonnegative Lagrange multipliers. The optimal separating hyperplane is obtained as a linear combination of training vectors:

$$\mathbf{w} = \sum_{i=1}^l \lambda_i y_i \mathbf{x}_i \quad (16)$$

Once the solution is found, \mathbf{x}_i 's having $\lambda_i \neq 0$ are called as the *support vectors*. The hypothesis space can be expressed as:

$$f(\mathbf{x}) = \text{sgn}(\mathbf{w} \cdot \mathbf{x} + b) = \text{sgn}\left(\sum_{i=1}^l y_i \lambda_i (\mathbf{x} \cdot \mathbf{x}_i) + b\right) \quad (17)$$

In the case of separating the linearly non-separable samples by a linear surface, that is allowing some errors in order to be able to solve the problem by a linear function, a penalty proportional to the amount of constraint violations is introduced, leading to a soft margin classifier:

$$\begin{aligned} \min \quad & \Phi(\mathbf{w}, \Xi) = \frac{1}{2} \|\mathbf{w}\|^2 + C \left(\sum_i \xi_i \right)^k \\ \text{s.t.} \quad & y_i (\mathbf{w} \cdot \mathbf{x}_i + b) \geq 1 - \xi_i \\ & \xi_i \geq 0 \end{aligned} \quad (18)$$

In the equation above ξ_i are the penalty variables associated with each vector and C and k are parameters defining the cost of constraints violation. Thus, the Lagrange functional constructed for this problem has the following form:

$$L(\mathbf{w}, b, \Lambda, \Xi, \Gamma) = \frac{1}{2} \|\mathbf{w}\|^2 - \sum_{i=1}^l \lambda_i [y_i (\mathbf{w} \cdot \mathbf{x}_i + b) - 1 + \xi_i] - \sum_{i=1}^l \gamma_i \xi_i + C \left(\sum_{i=1}^l \xi_i \right)^k \quad (19)$$

Similarly, the saddle point of the above equation gives the solution:

$$\mathbf{w} = \sum_{i=1}^l \lambda_i y_i \mathbf{x}_i \quad (20)$$

and the hypothesis space is expressed as:

$$f(\mathbf{x}) = \text{sgn} \left(\sum_{i=1}^l y_i \lambda_i (\mathbf{x} \cdot \mathbf{x}_i) + b \right). \quad (21)$$

In both of the above problems, it can be seen that the hypothesis space expansion is described in terms of dot products between the data. This feature will be useful for solving the nonlinear separation problem.

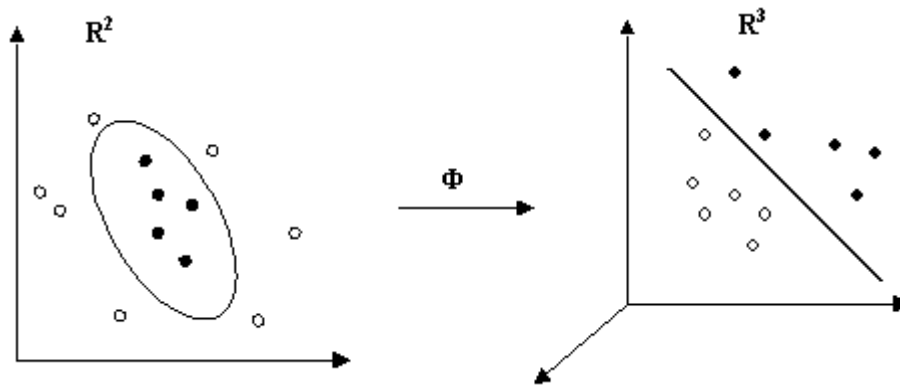


Figure 13 By mapping the nonlinearly separable input data into a higher dimensional feature space, the data can be separated by a linear decision surface.

The most important feature of the SVM is the use of the concept of kernels. To be able to incorporate nonlinear separation, the input variable \mathbf{x} is mapped in a higher

dimensional feature space ($\mathbf{x} \rightarrow \Phi(\mathbf{x})$) where dot product is defined [40]. The linear classification rules can be applied in this higher dimensional space (see Figure 13). Since the solution of the SV optimization problem is in the form of dot products, x can be replaced by $\Phi(\mathbf{x})$, and a nonlinear algorithm can be obtained by using kernel functions.

Defining the kernel function as the inner product of the mapped samples

$$K(\mathbf{x}, \mathbf{y}) = \Phi(\mathbf{x}) \cdot \Phi(\mathbf{y}), \quad (22)$$

the following dual problem is constructed:

$$\begin{aligned} & \max \\ & \sum_i \lambda_i - \frac{1}{2} \sum_{i,j} \lambda_i \lambda_j y_i y_j K(\mathbf{x}_i, \mathbf{x}_j) \\ & \text{s.t.} \\ & 0 \leq \alpha_i \leq C \\ & \sum_i \lambda_i y_i = 0 \end{aligned} \quad (23)$$

Therefore, the only quantities that need to be computed are the scalar products of the feature vectors. There is no need to compute the mapping of the input vectors to another feature space. The decision function can be expressed as a function of the dot product of the mapped features, therefore it may as well be expressed in terms of the kernel function $K(\mathbf{x}, \mathbf{y})$. If $K(\mathbf{x}, \mathbf{y})$ is a function that can be computed easily, it is reasonable to use K instead of computing the mapping $\Phi(\mathbf{x})$. The class of a vector \mathbf{x} can be decided using (23) as

$$f(\mathbf{x}) = \text{sgn}\left(\sum_i \alpha_i K(\mathbf{x}, \mathbf{sv}_i) + b\right). \quad (24)$$

K should be a symmetric kernel that corresponds to a dot product in some feature space. This is satisfied if K is a function that satisfies Mercer's condition discussed in detail in [60]. Polynomials, radial basis functions (RBF) and certain sigmoid functions are among the suitable kernel functions:

$$\begin{aligned} \textit{Polynomial} : K(\mathbf{x}, \mathbf{y}) &= (a\mathbf{x} \cdot \mathbf{y} + b)^p \\ \textit{Gaussian(RBF)} : K(\mathbf{x}, \mathbf{y}) &= e^{-\frac{\|\mathbf{x}-\mathbf{y}\|^2}{2\sigma^2}} \\ \textit{Sigmoidal} : K(\mathbf{x}, \mathbf{y}) &= \tanh(a\mathbf{x} \cdot \mathbf{y} - b) \end{aligned} \quad (25)$$

For the linear SVMs, K is the polynomial kernel with $a=1$, $b=0$, and $p=1$.

The ANSI C++ code library LIBSVM [10] is used to build the support vector experiments in this study.

CHAPTER V

RESULTS

5.1 Data Set

The data used in this study has been recorded during the sleep experiments performed at the Sleep Research Center in the Department of Psychiatry of Gülhane Military Medical Academy (GATA). A digital polysomnograph (Somno Star Alpha) was used to collect the sleep data. Silver plated surface electrodes were used. 16 channels of EEG, EOG from both eyes, EMG from the chin and both legs, respiration and ECG data were recorded for all subjects. EEG data were obtained from 16 derivations attached to the head according to the 10-20 system unipolarly, taking the A1 and A2 channels as references.

The high-pass filter was set at 0.5 *Hz* and the low-pass filter at 50 *Hz*, so that only the signals in the 0.5-50*Hz* band are recorded. The notch filter was on to eliminate noise due to the main power system. The sampling rate was 200 *Hz* with 8 *bit* resolution. EMG and EOG data were also recorded with 200 *Hz* sampling rate.

The recordings were taken for at least two consecutive nights, and the data of the second night was used for all subjects as the baseline sleep.

Whole night sleep of two insomniac and two healthy male subjects were studied. The ages of the subjects ranged from 17 to 25 years. The subjects were asked to answer a

set of questions at the night of the experiment, prior to sleeping. The subjects went to sleep when they were sleepy. The recording started when the subject lay down and lasted until the termination of sleep.

All channels of the polysomnograph were used for visual stage scoring done by the experts. For training the classifiers, we analyzed the whole night sleep of an insomniac and two healthy subjects in this study. The total recording of the insomniac subject consisted of 689 epochs, and those of the healthy subjects consisted of 708 epochs and 822 epochs, each epoch corresponding to 30 *sec* of sleep recording. Sleep spindles can most easily be observed on the central electrodes, therefore sleep spindles in stage 2 sleep of the subjects were marked visually using C3-A2 channel by an expert. Another expert reviewed the marked regions to eliminate subjectivity.

Sleep spindles may be formed due to two causes. The activity occurs sometimes as a response to a stimulus and sometimes as a spontaneous activity of the thalamus. Stage 2 sleep is the most dominant stage of sleep. The 45 to 60 % of the sleep of a healthy adult consists of stage 2. In the sleep pattern, along with stage 2 sleep lasting only for a few minutes, there are also stage 2 sleep present that lasts several minutes without interruption. It is more likely that the sleep spindle occurrences in the stage 2 sleep that lasts only a few minutes are of the first kind, that is, a response to a stimulus. However, when a stage 2 period that continues for at least 20 minutes is considered, the spindle activity in this period could be defined as the spontaneous type of spindle occurrence. The spindles that are evoked responses may have different formation than the spontaneously occurring types.

The main purpose of this study is the assessment of the spontaneously occurring spindles. For this reason, while studying the healthy subjects, the stage 2 sleep, which continued at least for 20 minutes without interruption, was examined. Besides, the spindles that were close to the k-complexes or any other transient waveforms were excluded.

Similarly, in the study of the insomniac subjects, only the sleep spindles that were isolated from the k-complexes or any other transient waveform were marked but the criterion on stage 2 length was not set.

5.2 Feature Extraction

STFT and AR modeling were used as the feature extraction methods to demonstrate that not only the widely used frequency domain characteristics but also the time domain characteristics of the EEG can be used as features to differentiate between the different rhythms and to find out which method was more advantageous to use.

5.2.1 STFT

Selecting the type and the duration of the window function is an important issue in STFT since it determines the time and frequency resolution of the transform. Hamming window was used as the windowing function of STFT since it is a broadly used window function in EEG analysis. A set of experiments has been conducted in order to find an appropriate window length to represent the features of the data. The 500 *msec* window was found to give the best results. It is worthy to note here that being at least 500 *msec* duration is in the definition of sleep spindles [44]. Shorter windows gave poorer results since they classified other high frequency transients that

were not spindles as being spindles. The longer windows gave poorer results since the power contribution of the spindle was suppressed by the low frequency-high amplitude background activity when the spindle duration was around 500 *msec*. Therefore, in the rest of the experiments the features obtained by 500 *msec* Hamming window were used.

STFT was applied on the regions of the C3-A2 channel which were marked according to the criteria explained in the previous section. From the transformed data, the feature vectors were formed by using the 32 coefficients between 2 and 64 *Hz* and a target value was assigned to each feature implying whether it is a spindle or not (1=spindle, -1=not spindle).

In this way, 1750 samples for the insomniac subject and 484 samples for one of the healthy subjects were generated with equally distributed spindle and non-spindle samples. These feature sets were used in training the classifiers therefore the number of features belonging to the spindle regions and the non-spindle regions needed to be equal. For the second healthy subject, there was no such constraint since it was used only for testing, thus 351 samples belonging to the spindle regions and 789 to the non-spindle regions were generated. It should be noted that the window used in STFT is shifted along the EEG data with steps less than the window length, therefore more than one sample might be obtained for the same spindle region.

A stage 2 signal of length 1000 samples (i.e. 5 *sec*) interval is given in Figure 14.a. The Hamming window of length 100 samples (i.e. 500 *msec*) applied at $t=1.95$ *sec* (where a spindle is present) is shown in Figure 14.b. Figure 14.c shows the

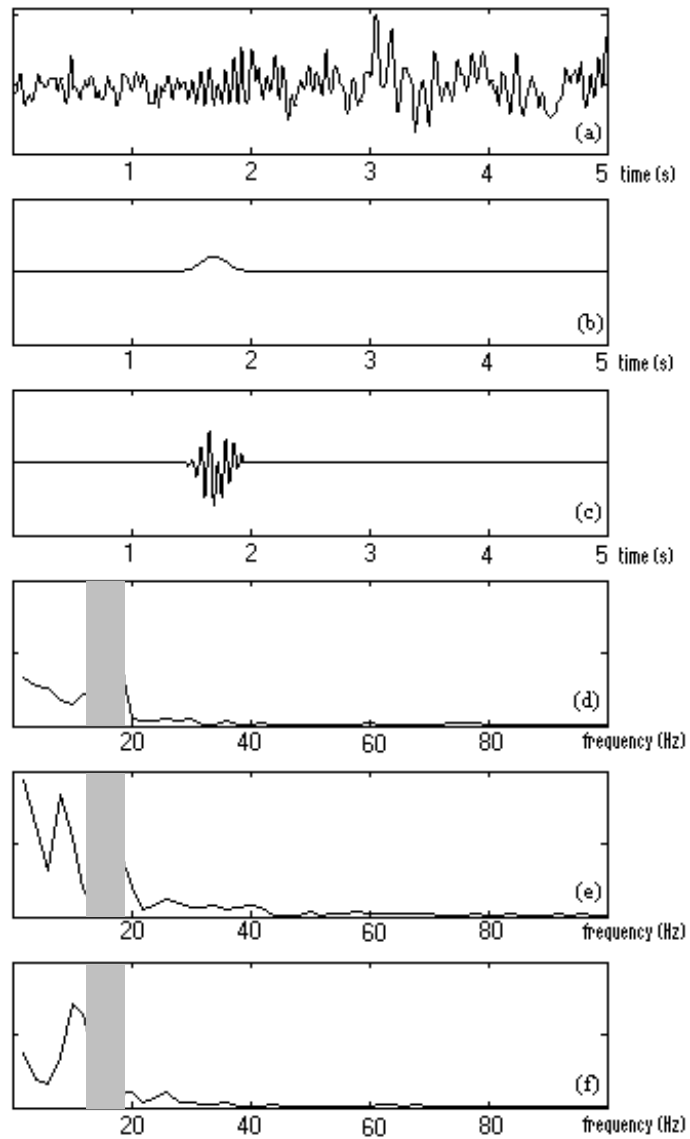


Figure 14 Stage 2 EEG and STFT a) original signal for 5 *sec* interval, b) Hamming window of length 500 *msec* ($M=100$) applied at $t=1.95$ *sec*, c) windowed signal, d) STFT (2-64 *Hz*) for a spindle region (the signal shown in (c)), e) STFT for a non-spindle region, f) STFT (2-64 *Hz*) for another non-spindle region. The shaded regions denote the spindle frequency range.

windowed signal. STFT (2-64 *Hz* interval) of the windowed signal shown in 14.c, which corresponds to a spindle region, is given in Figure 14.d. STFT for two different non-spindle regions are given in Figure 14.e and 14.f to demonstrate the power distribution of the spindle and non-spindle regions.

5.2.2 AR Modeling

Order selection is the most important decision to be made in signal modeling. There are some criteria that can be used for AR model order selection as discussed in section 3.2. However, due to the drawbacks of those criteria mentioned in [55] and since our purpose in this study is to extract features from the signals so as to give the best separable class of patterns, we did not use any such criteria. Instead, feature vectors using different model orders were formed and the classifiers were trained for each of these different sets to observe the performance over each model order. The feature vectors obtained by model order 12 and lower could not be classified at all, that is the performances over the training vectors for these model orders were around 50 %. The performance over the training set started to increase for feature vectors formed from higher model orders. However, the performance over the test set obtained by using model orders lower than 16 were poorer than the performance obtained by the model order 16. Additionally, the results obtained using model order 16 and higher were found to be similar. Therefore, the parameters of model order 16 were used as features.

In the experiments conducted on the insomniac subject, only a single feature was extracted for each spindle region by using AR modeling. This way 800 samples, 400 being for spindle regions and 400 for non-spindle regions, were generated for the

insomniac subject. However, the length of the total stage 2 sleep examined for the healthy subjects was shorter due to the criterion mentioned in section 5.1. Therefore, the number of marked spindle regions were much less for the healthy subjects (40 for one subject, 56 for the other) whereas there were 400 spindle regions marked for the insomniac subject. Thus, the features for the healthy subjects were extracted by sliding the 500 *msec* long analysis window by 100 *msec* steps like done in the STFT, allowing to extract more than one feature vectors for long spindle regions. This way, same number of spindle and non-spindle samples were generated as in STFT.

The spectrum of the autocorrelation function of the same EEG signal of Figure 14.a and that of the signal obtained by driving the filter (formed using the model parameters) with white noise are given in Figure 15, showing that the autocorrelation functions are successfully represented by the model.

5.3 Classification Results

Two different classifiers, namely MLP and SVM were employed in order to have comparative results and to validate the feature extraction methods used.

A different classifier for each feature set was trained to compare the performances achieved by each feature extraction method. However, it is known that the spindle formation differs in the presence of CNS disorders. Therefore, the detection systems for insomniac and healthy subjects would perform differently. Thus, we can speak of mainly two systems of spindle detection, one for the healthy subjects and another for the insomniac subjects. The first system was trained using the features extracted from one of the insomniac subjects and the second system was trained using the features extracted from a healthy subject.

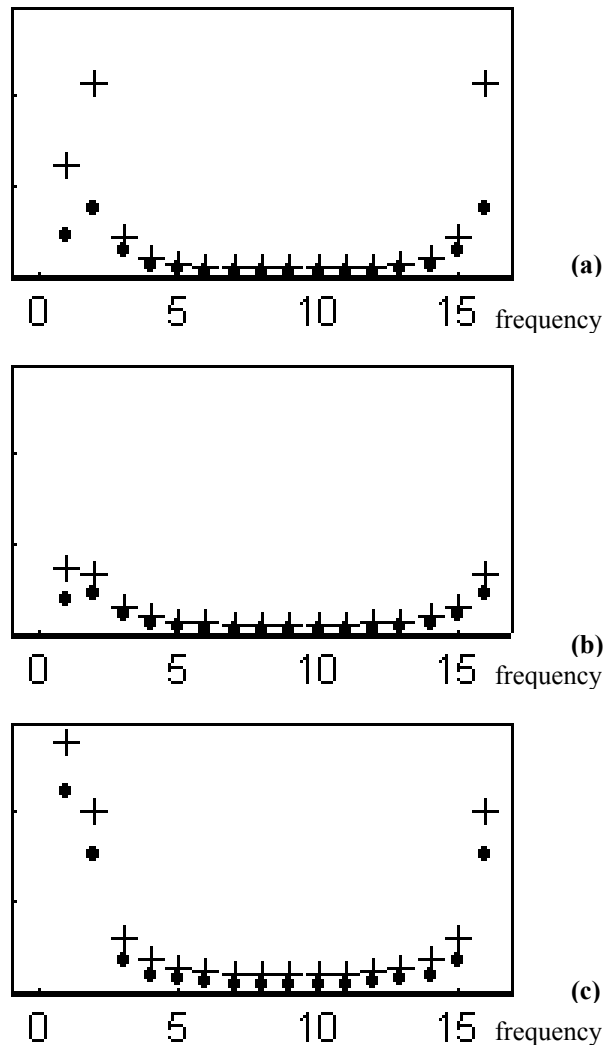


Figure 15 Spectrum of the autocorrelation function (i.e. $R_0 \dots R_p$) of the original signal (+) and the signal obtained by applying white noise to the input of the filter formed by the AR model parameters (•). a) a spindle region b) a non-spindle region c) another non-spindle region

The feature sets were not large, thus multi-fold experiments were conducted. The 1750 samples of the STFT feature set of the insomniac subject were divided into 10 folds, each fold being 175 feature vectors. 9 of 10 folds were used in training and the remaining one fold was used for testing (that is, the training set consisted of 1575 samples and the test set consisted of 175 samples). This was repeated 10 times by repeating each possible combination. The AR model feature set of the insomniac subject consisted of 800 samples, thus it was divided into 8 folds that consisted of 100 samples. Therefore, 8 experiments were conducted for each possible combination.

The feature set of the healthy subject that is used for training the second system consisted of 484 samples, thus the feature set was divided into 6 folds and 6 experiments were conducted considering each possible combination. The second healthy subject's data was used only for testing the second system performance, thus separation into folds was not necessary for this set.

The performances of the classifiers are given in the next two subsections, demonstrating the consistency and the reliability of the systems formed.

5.3.1 MLP

Three layer MLP structure was used in all experiments. The number of input neurons is determined by the size of the input feature vectors. There is no general rule for selecting the number of hidden neurons, thus it is determined experimentally. The size of the feature vectors formed using STFT was 32 and that of the feature vectors formed using AR modeling was 16. Adding 1 neuron for bias, the networks were formed with 33 input neurons, 60 hidden neurons, and 1 output neuron for the STFT

features and 17 input neurons, 30 hidden neurons and 1 output neuron for the AR model features. Tanh function is used as the activation function of all neurons for all networks. For all training sets, a disjoint cross validation set with same size as the test set was generated and used for stop criterion of training.

As mentioned above, the first system was trained using the features extracted from the EEG of one of insomniac subjects. The two feature extraction methods gave similar results. The average performance of the network trained with the STFT features was found to be 89.5% and that of the network trained with the AR model features is found to be 88.8%, that is, only 0.7% lower than the former. The performance of the network trained with the 10 fold STFT features is presented in Table II and the performance of the network trained with the 8 fold AR model features is presented in Table III.

Table II Test set results of MLP trained with the STFT features of the insomniac subject.

	STFT
Fold 1	93.7%
Fold 2	84.0%
Fold 3	87.4%
Fold 4	91.4%
Fold 5	93.1%
Fold 6	92.6%
Fold 7	90.9%
Fold 8	86.3%
Fold 9	89.7%
Fold 10	86.3%
Avg.	89.5%

Table III Test set results of MLP trained with the AR features of the insomniac subject.

	AR
Fold 1	99.0%
Fold 2	92.0%
Fold 3	96.0%
Fold 4	91.0%
Fold 5	81.0%
Fold 6	74.0%
Fold 7	89.0%
Fold 8	85.0%
Avg.	88.8%

This system was applied to the EEG of two consecutive nights' sleep of another insomniac subject to investigate the effects of a hypnotic on sleep spindle density. On the first night, the subject did not have any medication. On the second night, the subject was given a hypnotic medicine, which is known to increase the spindle density. The system detected almost 1/3 more spindle occurrences for the second night than the first night, hence the output of the MLP is concordant with the fact that the hypnotic increases spindle density. A sample for 6 *sec* duration of stage 2 sleep of the second sleep cycle for both nights is depicted in Figure 16. It is worth to mention that at least five consecutive positives denotes the presence of a spindle region since the window is shifted with 100 *msec* steps for extracting features and being at least of 500 *msec* duration is in the definition of spindles.

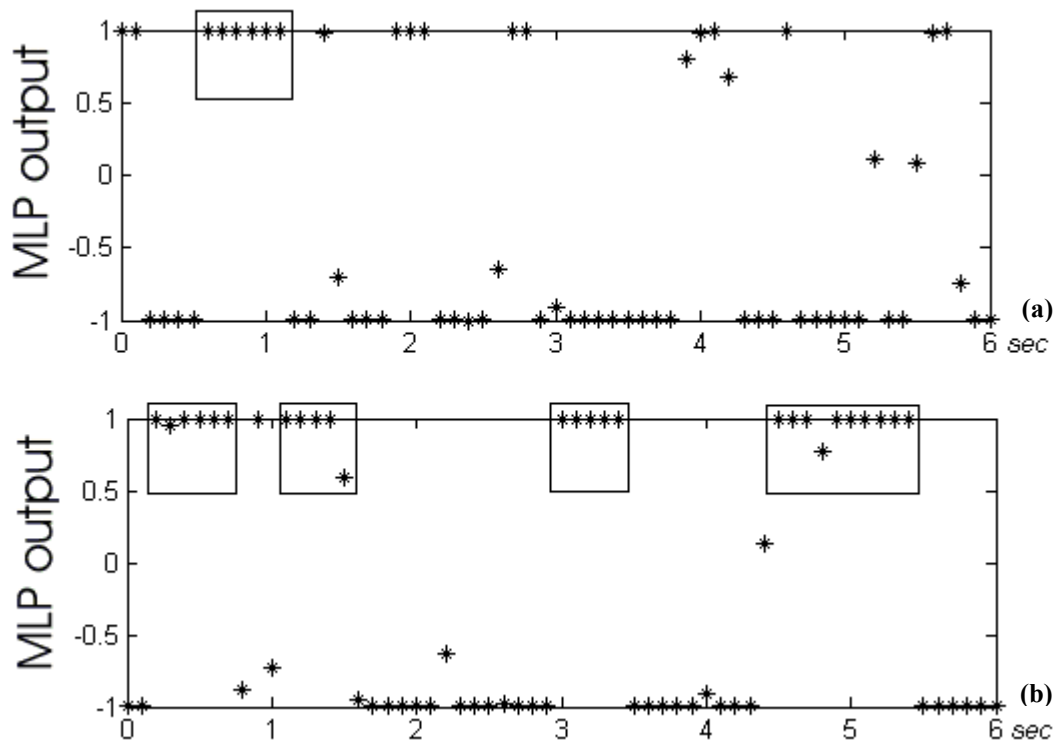


Figure 16 The output of MLP for 6 sec stage 2 sleep EEG (C3-A2) for the same subject recorded at two consecutive nights; a)with no medication, b) with hypnotic. (Horizontal axis is time, vertical axis is the output of MLP: $0.5 < \text{spindle} < 1$, $-1 < \text{not spindle} < -0.5$) The spindle regions are marked by the rectangles.

The second detection system was trained using the features extracted from one of the healthy subjects. The training was done on the 6 fold data as previously mentioned.

The two feature extraction methods resulted in high performances. The average performance of the network trained with the STFT features was found to be 97.5% and that of the network trained with the AR model features is found to be 93.6%. The

performances of the networks trained for the healthy subject using STFT and AR modeling are given Table IV.

Table IV Performances of the MLP networks trained using the features obtained by STFT and AR modeling from the healthy subject

	STFT	AR
Fold1	92.5 %	92.8 %
Fold2	100 %	91.3 %
Fold3	100 %	93.1 %
Fold4	100 %	95.9 %
Fold5	98.8 %	98.4 %
Fold6	93.8 %	90.0 %
Avg.	97.5 %	93.6 %

This system was tested on the samples of the other healthy subject to verify that the system could perform equally well on different healthy subjects. The performance of the system over the second healthy subject's features is given in Table V.

The spindle formation may be different in the presence of CNS disorders. When the system trained with the healthy subject's data was applied on the samples of the insomniac subject to test how well it would perform on a subject with CNS disorder, it was found that it performed poorly on the spindle regions as expected (see Table VI).

Table V Performances of the second MLP system on the other healthy subject (351 samples for spindle and 789 samples for non-spindle regions)

	STFT	AR
spindle	86.8 %	89.9 %
non-spindle	99.4 %	98.5 %
Avg.	93.1 %	91.7 %

Table VI Performances of the second MLP system on the insomniac subject (875 samples for spindle and 875 samples for non-spindle regions)

	STFT	AR
spindle	16.4 %	52.4 %
non-spindle	98.4 %	84.9 %
Avg.	57.4 %	68.6 %

5.3.2 SVM

SVM has been used as the second classifier to separate the spindle and non-spindle data to have comparative results and to validate the feature extraction methods used. Therefore, the SVM classifiers have been trained and tested with the same data used in the MLP. As done with the MLP, multi-fold data is used. Both the insomniac and the healthy subjects' EEG recordings were investigated using SVM. Polynomial and Gaussian (RBF) kernel functions were tested to achieve the best performance.

For the feature vectors formed by using STFT of the insomniac subject's EEG, Gaussian kernel performed the best. We set $C=100$ and repeated the experiments for varying values of γ as 0.25, 0.5, 1, 1.25, 1.5, and 2 where $\gamma = \frac{1}{2\sigma^2}$. We obtained the best result for $\gamma=1.25$ (Table VII). The average accuracy of the SVM was found to be 95.4 %, validating the MLP results.

Table VII SVM test set results on STFT features of the insomniac subject. (Gaussian kernel with $C=100$, and $\gamma=1.25$)

	STFT
Fold 1	97.7 %
Fold 2	93.7 %
Fold 3	95.4 %
Fold 4	95.4 %
Fold 5	97.1 %
Fold 6	96.0 %
Fold 7	94.9 %
Fold 8	93.1 %
Fold 9	94.9 %
Fold 10	96.0 %
Avg.	95.4 %

Similarly, different kernels were tested for the feature set formed with the AR model parameters for the insomniac subject. The best result was obtained using the linear SVM with average accuracy of 93.3 % (see Table VIII).

Table VIII SVM test set results on AR features of the insomniac subject (Linear SVM, C=100).

	AR
Fold 1	91.8 %
Fold 2	94.2 %
Fold 3	94.0 %
Fold 4	92.4 %
Fold 5	93.8 %
Fold 6	93.8 %
Fold 7	94.6 %
Fold 8	91.6 %
Avg.	93.3 %

The same procedure as in MLP was followed for the classification of the healthy subject's data. The training was done on the 6 fold data of the first healthy subject. Different kernel functions and C values were tested and the ones giving the best performance was taken. For the classifier trained with the STFT features, the best performance was achieved for the when the Gaussian kernel with $\gamma=0.125$ was used and C was set to 500. The average performance of the classifier was found to be 97.5 %.

For the AR model features, the Gaussian kernel with $\gamma=0.125$ gave the best results when was C taken as 50. The average performance of the classifier trained with the AR model features is found to be 94.4%. The performances of the classifiers trained with the 6 fold STFT and 6 fold AR model features is presented in Table IX.

Table IX Performances of the SVMs (Gaussian kernel with $\gamma=0.125$) trained using the 6 fold features obtained from a healthy subject by STFT (C=500) and AR modeling (C=50).

	STFT	AR
Fold1	97.5 %	96.3 %
Fold2	98.8 %	95.1 %
Fold3	98.8 %	96.3 %
Fold4	96.3 %	96.3 %
Fold5	97.5 %	91.4 %
Fold6	96.3 %	91.4 %
Avg.	97.5 %	94.4 %

Similarly, this system was tested on the samples of the other healthy subject. The performances of both classifiers over the second healthy subject's data are also found to be high, validating the MLP results. The performances over the spindle and non-spindle regions are presented in Table X.

Table X Performances of the second SVM system on the other healthy subject (351 samples for spindle and 789 samples for non-spindle regions)

	STFT	AR
spindle	90.6 %	92.9 %
non-spindle	99.2 %	99.2 %
Avg.	94.9 %	96.0 %

When the same system was applied on the samples of the insomniac subject to test how well it would perform on a subject with CNS disorder, however, it was found that the classifier that used STFT features performed poorly on the spindle regions as expected but that the classifier that used AR model features performed unexpectedly high on spindle regions (see Table XI).

Table XI Performances of the second SVM system on the insomniac subject (875 samples for spindle and 875 samples for non-spindle regions)

	STFT	AR
spindle	10.9 %	86.4 %
non-spindle	99.3 %	82.1 %
Avg.	55.1 %	84.2 %

CHAPTER VI

CONCLUSION

Sleep studies can improve our insight about the mechanism of the brain. Being one of the well-defined and functional rhythmic activities observed in sleep EEG, sleep spindles are significant for brain research.

Scientists assume that there is a close relationship between the spindle structure and brain maturation. Besides, sleep spindles are useful for classification of the NREM sleep and to evaluate the degree of arousal. The amount and distribution of the sleep spindles can be used to describe the morphology of the sleep EEG. Therefore, assessment of the distribution of sleep spindles over the whole night sleep is important. Being lower amplitude than the background EEG activity, some spindles are hard to be detected by the experts. Thus, the visual detection would not be objective. Additionally, the detection of each spindle occurrence in a whole night's sleep is very time consuming and tiring for the expert. Thus, an automated system for sleep spindle detection would reduce the workload of the expert and eliminate the subjectivity.

This work is aimed to build a reliable automated spindle detection system for practical use in the sleep research centers. For this purpose, two different classifiers,

MLP and SVM have been used to detect the spindle activity to have comparative results. It was shown that both feature extraction methods, STFT and AR modeling, could be used to successfully detect the spindle occurrences. The performances are presented in chapter 5, from Table II to Table XI.

In all experiments, the performances of the SVM classifiers were higher than that of the MLP classifiers. This was an expected result since it is known that MLP separates the input patterns with *some* hyperplane while SVM finds the *optimal* separating hyperplane.

The high performances achieved using different classifiers prove that both feature extraction methods are reliable. Using AR modeling, the dimension of the classifiers could be significantly reduced however, the performances of the classifiers formed by using the AR model features are lower than those of the classifiers trained by the STFT features both for MLP and SVM. Thus, we can conclude that although AR model parameters provide a good representation of the EEG data, STFT characterizes the features for discriminating the spindle and non-spindle regions better.

We have mentioned that spindles are formed due to two causes; as a spontaneous activity of the thalamus and as an event related phenomenon. The main purpose of this work is the assessment of the spontaneously occurring spindles thus, for both healthy and insomniac subjects, only the spindles that were isolated from the k-complex activity were marked. While extracting features from the healthy subjects' EEG, only the stage 2 sleep that continued for 20 minutes without interruption was examined, but there was no such criterion set while examining the insomniac subject's EEG. Therefore, it is probable that the marked spindle activity for the

healthy subjects are only of the spontaneously occurring type but some event related spindles are also included in the insomniac subject's samples. The higher performances of the classifiers trained by the healthy subject's data supports this assumption.

The classifiers trained by the healthy subject's data were simulated with the features obtained from another healthy subject, and the average performances over the spindle and the non-spindle regions were found to be high for both SVM (94.9%) and MLP (93.1%) trained with STFT features. The results obtained with AR model features are similarly high for both MLP (91.7%) and SVM (96.0%). Since spindle formation varies in the presence of CNS disorders, low performance over the spindle regions and high performance over the non-spindle regions was expected from both MLP and SVM when tested on the features extracted from the insomniac subject by both feature extraction methods. With MLP, the performances over the spindle regions were found to be low (16.4% for STFT and 51.1% for AR model) whereas the performances over the non-spindle regions were still high (99.2% for STFT and 88.9% for AR model) as expected. These results are concordant with the assumption that the sleep spindle characteristics do not vary for subjects in the same age group but the characteristics are influenced by the CNS disorders. The SVM classifiers gave similar results for the STFT features (10.9% on spindle regions and 99.2% on non-spindle regions). However, the performance of the SVM over the AR model features was found to be unexpectedly high (84.2%) on the spindle regions of the insomniac. This is a result that needs to be further investigated.

The MLP network trained by the feature set formed from the STFT coefficients was used to analyze the effect of a hypnotic on the spindle density of an insomniac

subject. It was observed that the hypnotic enhanced the spindle density, which is a well-known fact, demonstrating that the recognition of the spindles could be clearly made and that the method is reliable.

In this thesis, only the detection of the spindles was implemented. Our next objective is the assessment of the relation of the spindle activity with the background EEG activity is also important in describing the morphology of sleep. It is known that there are two kinds of sleep spindle activity. One kind occurs as a spontaneous activity of the thalamus and the other as an evoked response to stimuli. Thus, the sleep spindles are examples of both spontaneous and event related oscillations of the brain. For this reason, evaluating and analyzing the characteristics of the different kinds of spindles is also worth studying.

REFERENCES

- [1] Agarwal R., Gotman J., "Computer-assisted sleep staging," *IEEE Trans. on Biomedical Engineering*, Vol. 48, No. 12, 2001 pp.1412-1423
- [2] Akay M. (ed.), *Nonlinear biomedical Signal Processing* Vol. 1, New York: IEEE, 2000
- [3] Akgül T., Sun M., Sciabassi R., Çetin A.E., "Characterization of sleep spindles using higher order statistics and spectra," *IEEE Trans. on Biomedical Engineering*, Vol. 47, No. 8, 2000, pp. 997-1009.
- [4] Akın A., Akgül T., "Detection of sleep spindles by discrete wavelet transform," *Proceedings of the IEEE 24th Annual Northeast Bioengineering Conference*, 1998, pp. 15 -17
- [5] Asserinsky E., Kleitman N., "Regularly occurring periods of ocular motility and concomitant phenomena during sleep," *Science*, No 118, 1953, pp. 361-375.
- [6] Başar E., *Brain Function and Oscillations Vol. I: Brain Oscillations. Principles and approaches*, Springer-Verlag, Berlin, 1998
- [7] Burges C.J.C., "A Tutorial on Support Vector Machines for Pattern Recognition," *Data Mining and Knowledge Discovery*, Vol. 2, No. 2, 1998, pp. 121-167.
- [8] Campbell K., Kumar A., Hofman W., "Human and automatic validation of a phase-locked loop spindle detection system," *Electroencephal Clin Neurophysiol*, Vol. 48, 1980, pp. 602-605
- [9] Caspary O., Nus P., Devillard F., "Spectral analysis methods applied to sleep spindles," *Proc. ICSPAT'96*, Boston, USA, Vol. 1, 1996, pp. 374-378.
- [10] Chang C.C. and Lin C.J., *LIBSVM : A library for support vector machines*, 2001
- [11] Clemens B., Menes A., "Sleep spindle asymmetry in epileptic patients," *Clinical Neurophysiology*, Vol.111, 2000, pp. 2155-2159.
- [12] Contreras D., Destexhe A., Sejnowski T.J., Steriade M., "Spatiotemporel patterns of spindle oscillations in cortex and thalamus," *The Journal of Neuroscience*, Vol. 17(3), 1997, pp. 1179-1196.
- [13] Cote K.A., Epps T.M., Campbell K.B., "The role of the spindle in human information processing of high-density stimuli during sleep," *Journal of Sleep Research*, Vol. 9, 2000, 19-26
- [14] De Gennaro L., Ferrara M., Bertini M., "Effect of slow-wave sleep deprivation on topographical distribution of spindles," *Behavioral Brain Research*, No. 116, 2000, pp. 55-59.

- [15] De Gennaro L., Ferrara M., Bertini M., "Topographical distribution of spindles: Variations between and within NREM sleep cycles," *Sleep Research Online* 3(4): 2000, pp. 155-200.
- [16] Destexhe A., Contreras D., Steriade M., "Cortically-induced coherence of a thalamic-generated oscillation," *Neuroscience*, Vol. 92, 1999, pp. 427-443.
- [17] Dijk D.J., "EEG slow waves and sleep spindles: windows on the sleeping brain," *Behavioural Brain Research*, Vol. 69, 1995, pp.109-116.
- [18] Duda R.O., Hart P.E, Stork D.G., *Pattern Classification*, 2nd ed. New York: John Wiley and Sons, 2001
- [19] Durka, P.J., *Time-Frequency analysis of EEG*, PhD Thesis, Warsaw University, August 1996
- [20] Eroğul O., Bahadırlar Y., Güler Ç., Aydın H., "Parametric analysis of the sleep spindles by using matching pursuit method," *National Meeting of Biomedical Engineering*, October 1999, Kayseri, Turkey (in Turkish)
- [21] Eroğul O., Güler Ç., Bahadırlar Y., Aydın H., "A method for detection and analysis of the spindles in sleep EEG," *National Meeting of Biomedical Engineering*, October 1999, Kayseri, Turkey (in Turkish)
- [22] Ficca G., Fagioli I., and Salzarula P.: *Sleep organization in the first year of life: Developmental trends in the quiet sleep-paradoxical sleep cycle*, J Sleep Res, Vol. 9, 2000, pp. 1-4
- [23] Finelli L.A., Achermann P., Borbely A.A., "Individual 'fingerprints' in human sleep EEG topography," *Neuropsychopharmacology*, Vol. 25, No. S5, 2001 pp. 57-62.
- [24] Gath I., Inbar G.F. (ed.), *Advances in Processing and Pattern analysis of biological signals*, 1996 Plenum Press, New York
- [25] Görür D., Halıcı U., Aydın H., Ongun G., Özgen F., Leblebicioğlu K., "Sleep spindles detection using short time Fourier transform and neural networks," *Proc. IJCNN 2002*, Hawaii, USA, 2002, pp. 1631-1636.
- [26] Guyton A.C, *Textbook of medical physiology*, 8th ed., 1991, PA: Saunders Company
- [27] Hazarika N., Chen J.Z., Tsoi A.C, Sergejew A., "Classification of EEG signals using the wavelet transform," *Signal Processing*, Vol. 59, 1997, pp. 61-72.
- [28] Hearst M.A., "Support Vector Machines", *IEEE Intelligent Systems*, 1998, pp. 18-28.
- [29] Himanen S.L, *A New Visual Adaptive Scoring System for Sleep Recordings. Development and Application of the Multiple Sleep Latency Test*, PhD Thesis, Tampere University, 2000
- [30] Kandel E.R., Schwartz J.H., Jessell T.M., *Principles of Neural Science*. 4th ed., McGraw-Hill Professional Publishing, 2000

- [31] Kay S.M., *Modern Spectral Estimation: Theory and Application*, NJ: Prentice-Hall, 1988
- [32] Kohsaka S., Sakai T., Kohsaka M., Fukuda N., Kobayashi K., "Dual control of the brainstem on the spindle oscillation in humans," *Brain Research*, Vol. 882, 2000, pp. 103-111.
- [33] Kubicki S., Herrmann W.M., "The future of computer-assisted investigation of the polysomnogram: Sleep microstructure," *J Clin Neurophysiology*, Vol.13, 1996, pp. 285-294.
- [34] Levin K.H., Lüders H.O., *Comprehensive Clinical Neurophysiology*, Saunders Company, 2000, USA
- [35] Louis J., Zhang J.X., Revol M., Debilly, and Challamel M.J., "Ontogenesis of nocturnal organization of sleep spindle: a longitudinal study during the first 6 months of life," *Electroencephal Clin Neurophysiol*, Vol. 83, 1992, pp. 289-296.
- [36] Nicolas A., Petit D., Rompre S., Montplaisir J., "Sleep spindle characteristics in healthy subjects of different age groups," *Clinical Neurophysiology*, Vol. 112, 2001, pp. 521-527.
- [37] Ogilvie R.D., "The process of falling asleep," *Sleep Medicine Reviews*, Vol. 5, 2001, pp. 247-270.
- [38] Oppenheim A.V., Schafer R.W, Buck J.R, *Discrete-Time Signal Processing*, 2nd ed., 1999, New Jersey: Prentice Hall
- [39] Oropesa E., Cycon H.L., Jobert M., "Sleep stage classification using wavelet transform and neural network," *International Computer Science Institute*, TR-99-008, March 1999
- [40] Osuna E., Freund R., and Girosi F., "An Improved Training Algorithm for Support Vector Machines", *Proc. IEEE Workshop on Neural Networks for Signal Processing*, 1997.
- [41] Pardey J., Roberts S., Tarassenko L., "A review of parametric modeling techniques for EEG analysis," *Med. Eng. Phys.*, Vol. 18, 1996, pp. 2-11.
- [42] Pivik R.T., Bylisma F.W., Nevins R.J., "A new device for automatic sleep spindle analysis: The Spindicator," *Electroencephal Clin Neurophysiol*, Vol. 54, 1982, pp. 711-713
- [43] Pivik R.T., Joncas S., Busby K.A., "Sleep spindles and arousal: The effects of age and sensory stimulation," *Sleep Reserach Online*, Vol. 2, 1999, pp. 89-100.
- [44] Rechtschaffen A., Kales A. (Eds.), *A manual of standardized terminology, techniques and scoring system for sleep stages of human subjects*, Brain Research Institute, UCLA, Los Angeles, USA, 1968
- [45] Roberts S., Tarassenko L., "Analysis of the sleep EEG using a multilayer network with spatial organization," *IEE Proceedings-F*, Vol. 139, 1992, pp. 420-425.

- [46] Roth C., Achermann P., Borbely A. A., "Alpha activity in the human REM sleep EEG: topography and effect of REM sleep deprivation," *Clinical Neurophysiology*, Vol. 110, 1999, 632-635
- [47] Rumelhart D.E., Hinton G. E., and Williams R. J., "Learning internal representations by error propagation," in *Parallel Distributed Processing: Explorations in the Microstructure of Cognition* (Rumelhart D.E., and J. L. McClelland, eds.), Vol.1, Chapter 8, Cambridge, MA: MIT Press, 1986
- [48] Schlögl A., Anderer P., Roberts Sleep.J., Pgegenzer M., Pfurtscheller G., "Artefact detection in sleep EG by the use of Kalman filtering", *Proceeding of the EMBEC '99*, pp. 1648-1649.
- [49] Smola A.J., *Learning with Kernels*, PhD thesis, Technische Universität Berlin, 1998.
- [50] Steriade M., Contreras D., Amzica F.: *Synchronized sleep oscillations and their paroxysmal developments*, Trends Neurosci, Vol. 17, 1994, pp. 199-208.
- [51] Steriade M., Deschênes M., "The thalamus as a neuronal oscillator," *Brain Res Rev*, Vol. 8, 1984, pp. 1-63.
- [52] Steriade M., Dossi R.C., Nunez A., "Network modulation of a slow intrinsic oscillation of cat thalamocortical neurons implicated in sleep delta waves: cortically induced synchronization and brainstem cholinergic suppression," *J Neurosci*, Vol. 11, 1991, pp. 3200-3217.
- [53] Sun M., Qian S., Yan X., Baumann S., Xia X., Dahl R., Ryan N., Sciabassi R., "Localizing functional activity in the brain through time-frequency analysis and synthesis of the EEG," *Proceedings of the IEEE*, Vol. 84, 1996, pp. 1302-1311.
- [54] Tagaya H., Trachsel L., Murck H., Antonijevic I., Steiger A., Holsboer Frequency., Friess E., "Temporal EEG dynamics of non-REM sleep episodes in humans," *Brain Research* 861, 2000, pp. 233-240.
- [55] Therrien C.W., *Discrete random signals and statistical signal processing*. Englewood Cliffs, NJ: Prentice-Hall, 1992
- [56] Tsoi A.C., So D.S.C., Sergejew A., "Classification of electroencephalogram using ANN," *Neural Information Processing Systems* 6, 1994, pp. 1151--1158
- [57] Ueda K, Nittono H., Hayashi M., Hori T., "Estimation of generator sources of human sleep spindles by dipole tracing method," *Psychiatry and Clinical Neurosciences*, Vol. 54, 2000, pp. 270-271.
- [58] Ueda K, Nittono H., Hayashi M., Hori T., "Spatiotemporal changes of slow wave activities before and after 14 Hz/12Hz sleep spindles during stage 2 sleep," *Psychiatry and Clinical Neurosciences*, Vol. 55, 2001, pp.183-184.
- [59] Vander A., Sherman J., Luciano D., *Human Physiology: The Mechanisms of Body Function*, 8th ed., 2001, New York: McGraw-Hill
- [60] Vapnik V.N., *The Nature of Statistical Learning Theory*, Springer, 1995.

- [61] Vaz F., De Oliveira P.G., Principe J.C., "A study on the best order for autoregressive EEG modelling," *Int. J. Bio-Medical Computing*, Vol. 20, 1987, pp. 41-50.
- [62] Vetterli M., Kovacevic J., *Wavelets and Subband Coding*. Upper Saddle River, NJ: Prentice-Hall, 1995
- [63] Williams R.L., Karacan I., Hirsch C.J., *Electroencephalography (EEG) of Human Sleep. Clinical Applications*. John Willey & Sons Inc. New York, 1974.
- [64] Woertz M., Schlögl A., Trenker E., Rappelsberger P., Pfurtscheller G., "Spindle filter optimization with receiver operating characteristics-curves," *Proceeding of the EMBEC '99*, pp. 480-481.
- [65] Zygierewicz J., *Analysis of sleep spindles and a model of their generation*, PhD thesis, Warsaw University, April 2000
- [66] Zygierewicz J., Blinowska K., Durka P.J., Szelenberger W., Niemcewicz S., Androsiuk W., "High resolution study of sleep spindles," *Clinical Neurophysiology*, No 110, 1999, pp. 2136-2147.